Article:
Sathsarani, HBS, Sampath, KHSM and Ranathunga, AS orcid.org/0000-0001-8746-5326 (2023) Utilization of fly ash-based geopolymer for well cement during CO2 sequestration: A comprehensive review and a meta-analysis. Gas Science and Engineering, 113. 204974. ISSN 2949-9097

https://doi.org/10.1016/j.jgsce.2023.204974

Manuscript Title: Utilization of Fly Ash-based Geopolymer for Well Cement during CO_2 Sequestration: A Comprehensive Review and a Meta-Analysis

Authors:

[1]H.B.S. Sathsarani, [1]*K. H. S. M. Sampath and [2]A. S. Ranathunga

[1]*Department of Civil Engineering, University of Moratuwa, Sri Lanka*

[2]*Department of Civil Engineering, School of Civil Engineering, University of Leeds, Leeds, UK*

Corresponding Author:

*K.H.S.M. Sampath

Lecturer, University of Moratuwa, Sri Lanka

sampathkh@uom.lk

Contact: +94701706017

ORCiD: 0000-0003-3605-4281

Abstract:

Global warming is a pressing issue caused by the increase in greenhouse gas emissions, with CO_2 contributing to 64% of total emissions. To reduce anthropogenic CO_2 emissions, several options have been proposed, including CO_2 sequestration. A key requirement for a successful and sustainable geo-sequestration process is the use of appropriate zonal isolation provided by the cementing material used between the annular surface and injection well. Although, Ordinary Portland Cement (OPC) is typically used as the well cement, it has shown failures during the process, including degradation issues, carbonation, shrinkage and microcracking, increased permeability in CO_2-rich environments, and loss of sealing properties in a short period of time. To address these problems, fly ash (FA)-based geopolymers have been introduced as a better well cement replacement. This study provides a comparative review between OPC and FA-based geopolymers in the context of CO_2 sequestration. The review comprehensively analyses the behaviour of FA-based geopolymer cement with its chemical composition, the impact of preparation conditions on the mechanical behaviour of geopolymers, and CO_2 permeability through FA-based geopolymer. Furthermore, a meta-analysis was conducted to develop statistical models for predicting the pertinent hydro-mechanical properties of FA-based geopolymer, including dry density, compressive strength, autogenous shrinkage strain, and CO_2 permeability during the geo-sequestration process. The outcomes of the meta-analysis can aid decision-making regarding the appropriateness of applying FA-based geopolymer as a replacement for OPC to conduct a sustainable and safe CO_2 geo-sequestration process under proper isolation conditions.

Keywords: CO_2 sequestration; Well cement; Ordinary Portland Cement; Fly ash; Hydro-mechanical properties

Graphical Abstract:

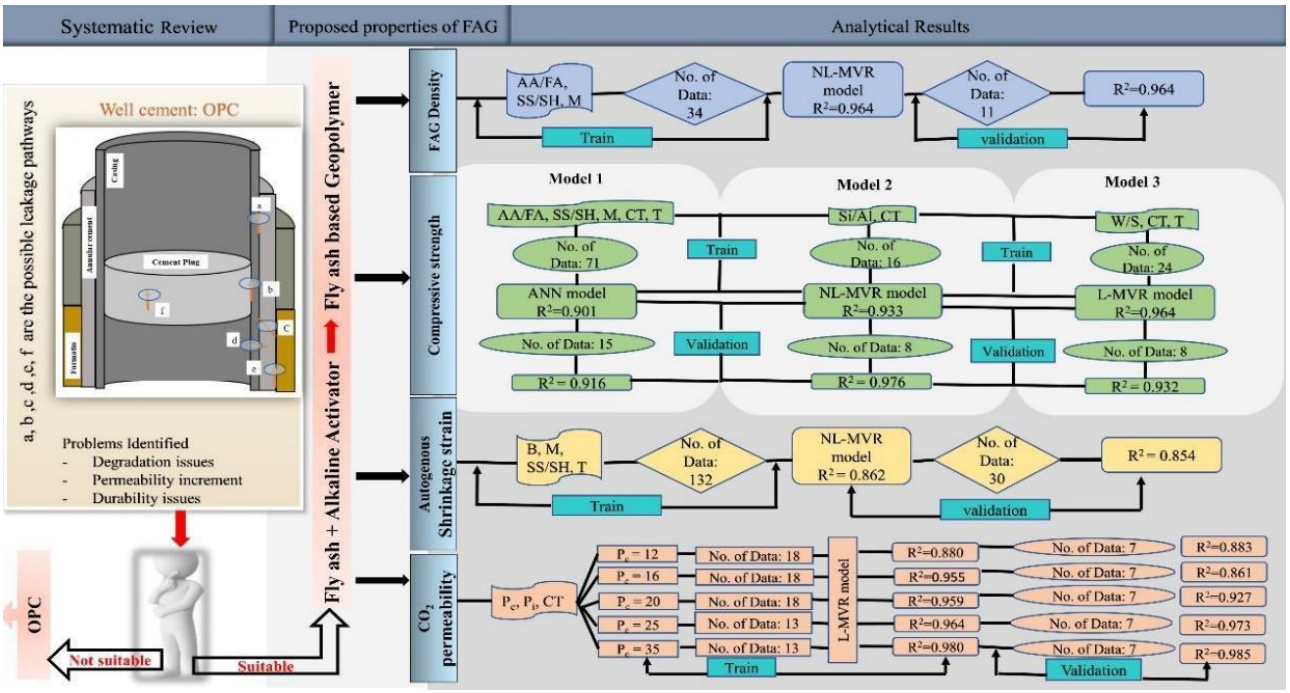

List of Abbreviations

AA/FA-Alkaline activator to Fly ash ratio
B – Binder (mass of fly ash and alkaline activator that is included in m^3 of FAG mixture)
CT – Curing Temperature(^{0}C)
L-MVR- Linear Multivariable Regression
M- NaOH concentration
NL-MVR -Non-Linear Multivariable Regression
P_c– Confining Pressure (Pa)
P_i – Injection Pressure (Pa)
SS/SH – NaOH to Na_2SiO_3 ratio
T – Curing time

Article Highlights

- Portland Cement and Fly Ash-based geopolymer are used as well cement for CO_2 sequestration.
- Their applicability is critically reviewed considering chemical and mechanical aspects.
- The superiority of Fly Ash-based geopolymer as a well cement is highlighted.
- Hydro-mechanical properties of Fly Ash-based geopolymer are statistically predicted.

Abbreviations

OPC	Ordinary Portland Cement
FA	Fly Ash
FAG	Fly Ash Geopolymer
API	American Petroleum Industry
GGBFS	Ground Granulated Blast Furnace Slag
XRF	X-Ray Fluorescence
XRD	X-Ray Diffraction
SEM	Scanning Electron Microscopy
EDX	Energy Dispersive X-ray
ASTM	American Society for Testing and Material
UCS	Uniaxial Compressive Strength
UTS	Uniaxial Tensile Strength
MVR	Multivariable Regression
L-MVR	Linear Multivariable Regression
NL-MVR	Non-Linear Multivariable Regression
ANN	Artificial Neural Network

1. Introduction

In the 20th and 21st centuries, fossil fuels are mostly used as power generation sources due to their vast availability. It fulfils about 82% of the world's energy requirement which is rapidly increasing due to the growth of the population (Newell et al., 2019). CO_2 is the main output of the burning of fossil fuels, which causes the acceleration of the global warming process by contributing 64% of total emissions of greenhouse gases (Bertier et al., 2006). China, the United States, the European Union, India, Russia, and Japan are the main CO_2 emitters in the world and at the end of 2020, the world's total fossil fuel-related CO_2 emissions ($FFCO_2$) were estimated about 34.8 billion tons of CO_2 (Karakurt & Aydin, 2023). As a result of finding a solution to reduce substantial anthropogenic CO_2 emissions, many options have been proposed. Some of them are; upgrading fossil fuels' efficiency and energy conversion, increasing interest in terrestrial and marine biomass, shifting energy production to low-carbon or non-carbon fuel sources, and CO_2 sequestration (Ji & Zhu, 2015). Among them, "CO_2 sequestration" can be considered one of the promising methods to address the issue. In the CO_2 sequestration process, the atmospheric CO_2 level is reduced by capturing and injecting the anthropogenic CO_2 into the underground deep geological settings including exhausted oil and gas pools, saline aquifers, sedimentary basins, and deep coal layers (Ji & Zhu, 2015; Sampath et al., 2020). In fact, anthropogenic CO_2 can be captured from mainly three types of activities: 1) industrial process, 2) electricity generation, and 3) hydrogen production (Kaldi et al., 2009). Figure 1 shows the capturing process of natural gas with high CO_2 content and preparing it for geo-sequestration. During the sequestration process, various gasses and oil trapped in deep aquifers can be extracted from the geological media and are produced from production wells. The injection of CO_2 into geo-reservoirs and the subsequent production of trapped oil/gas from aquifers without any leakages is a key requirement for this technique. The cementing material used in between the annular surface and injection well plays a major role in conducting a successful and sustainable geo-sequestration process by providing appropriate zonal isolation (Nasvi et al., 2013).

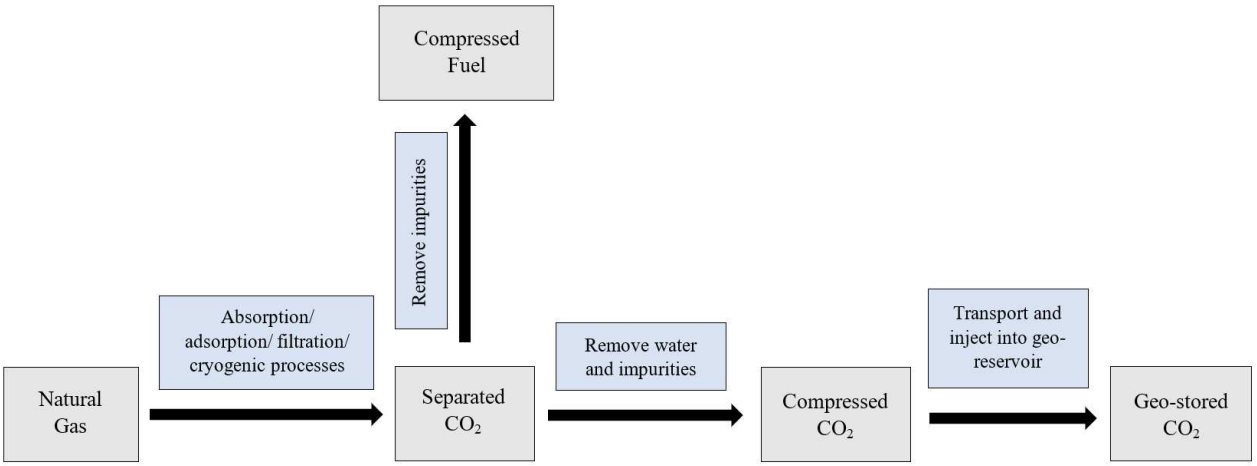

Figure. 1. Overview of carbon dioxide (CO_2) sequestration processes (Developed after Kaldi et al., 2009).

In general, Ordinary Portland Cement (OPC) is commonly used as well cement; however, it shows some failures in a CO_2-rich environment and loses its isolation properties within a short period of time (Nasvi et al., 2012a). Due to these reasons, geopolymer is introduced to replace Portland cement; among which, fly ash geopolymer (FAG) has a higher prominence due to its ability to reduce the gigantic amounts of fly ash (FA) piled up during coal-fired power plant operations (Hardjito et al., 2004). Figure 2 illustrates the production and the re-used amount of thermal power plant ash in different countries. The re-used percentages of FA in India, China, the UK, the USA, and Germany are quite low compared to the produced quantity, which signifies the importance of the utilization of this waste product in a productive manner (Ionescu & Lăzărescu, 2020). Therefore, the total dumps of FA that would lead to environmental pollution can be significantly minimized by encouraging the use of FA-based geopolymers as well cement during the CO_2 sequestration process. Thus, more focused research on the applicability of FA-based geopolymers, as a substitute to OPC for gas or well cementing during CO_2 sequestration is more essential.

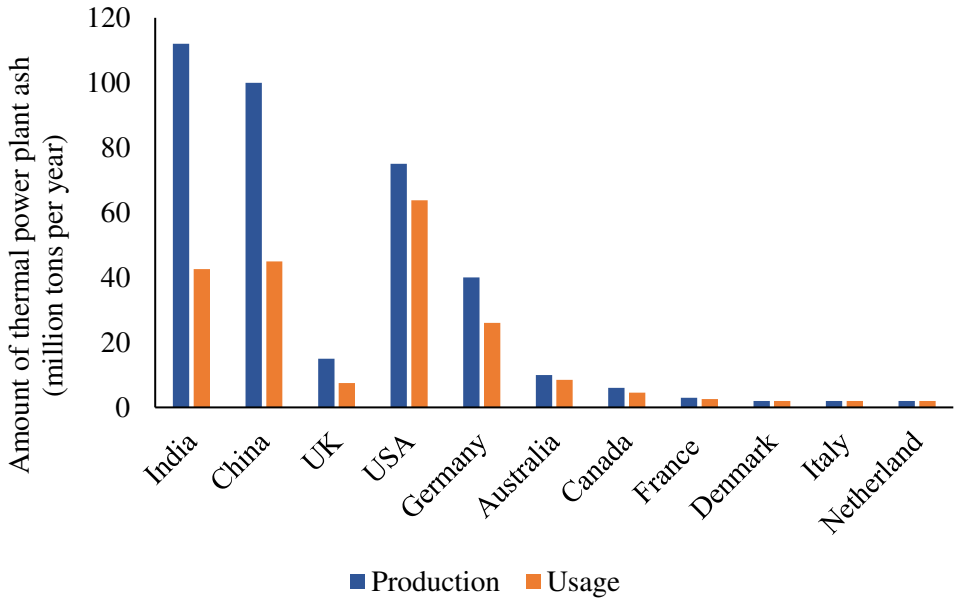

Figure. 2. Production and usage of thermal power plant ash in different countries (million tons per year) (Developed after Ionescu & Lăzărescu, 2020).

2. Review Methodology

This paper is mainly focused on comprehensively reviewing the literature on the following subcategories to identify the existing research gaps on the suitability of FA-based geopolymers as a replacement to OPC for well cementing during CO_2 sequestration.: 1) Role of well cement in a successful CO_2 geo-sequestration process, 2) OPC as a well cement and its problems, 3) FA-based geopolymers as an alternative well cement, highlighting the roles of alkaline activator, curing condition and temperature, 4) Mechanical behaviour of FA-based well cement including the variation in compressive strength, tensile strength, and permeability.

Figure 3 summarises the total number of publications reviewed in this study, including peer-reviewed journal publications, refereed conference publications, and research articles from different countries that are published over 36 years.

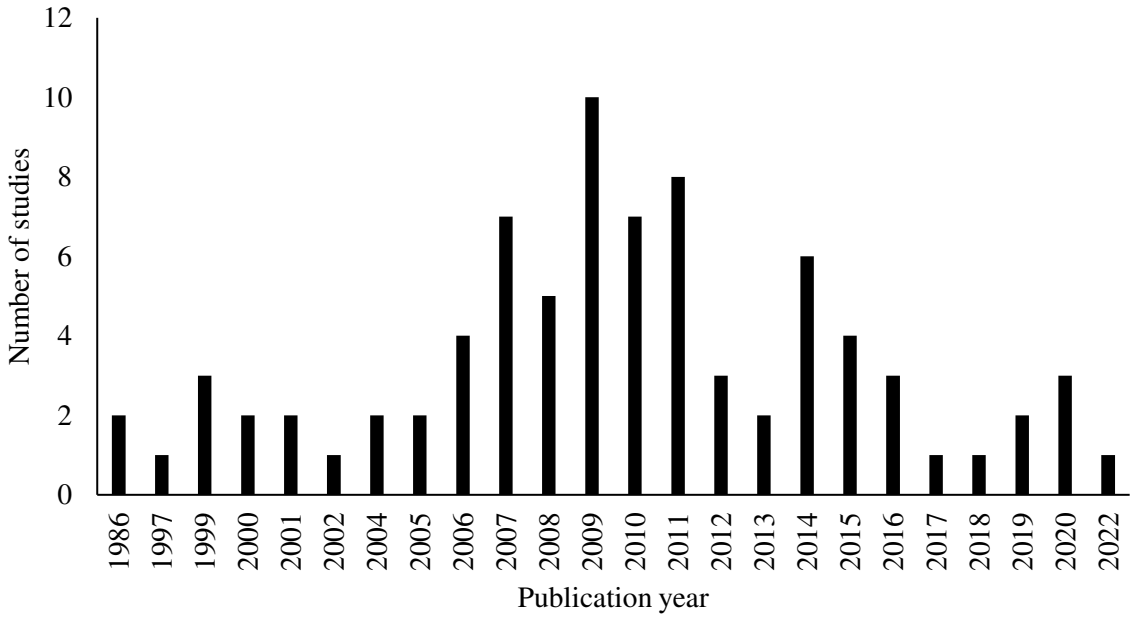

Figure. 3. Overview of the publication years of the reviewed studies.

3. Role of well cement in a successful CO_2 geo-sequestration process

Wellbore integrity is more important to conduct a successful CO_2 geo-sequestration process. For that, the leakage rate should be limited to 0.01% -1.0% per year, and if this rate is exceeded, it will be harmful to the groundwater table and the ecosystem in the surrounding (Kutchko et al., 2007). The cement that is used for wellbore integrity can be mainly divided into primary cement and secondary cement. The primary cement or annular cement fills the annular surface, connecting the casing and forming region, and the secondary cement material (i.e., cement plug) is poured inside the casing (refer to Figure 4) (Nasvi et al., 2013). This cementing material requires significant isolation characteristics to maintain a leakage-free wellbore, which include impermeability, non-shrinking ability, resistance to different chemicals, and ability to withstand mechanical loads (Khalifeh et al., 2014). The American Petroleum Industry (API) has classified different types of well cement, based on different temperature and pressure ranges. The most commonly available API class well cement types are listed in Table 1 (Robins & Milodowski, 1986). Based on the percentage content of tricalcium aluminate (C_3A), oil well cements are classified as 1) ordinary sulphate resistant, 2)

moderate sulphate resistant, and 3) high sulphate resistant well cements. Effective zonal isolation can be obtained by using the correct cement for specific well environments. In general, API classes of G and H, which are based on OPC have been used as well cement (Shahriar, 2011). However, with the variation of temperature and pressure conditions through the large depths, these well cements undergo radial cracking, durability issues, strength reductions, and permeability issues. These failure conditions may create leakage pathways in different ways through the wellbore and reduce the sealing capability with time (refer to Figure 5) (Nasvi et al., 2012a). In fact, temperature differences in the period of curing of cement, weak bonding between the cement and casing, and swelling and shrinkage of the cement during the curing period are the main reasons for generating the leakage pathways shown in Figure 5. Accordingly, the cement material that is used between the annular surface and wellbore plays a key role in achieving the appropriate isolation properties to carry out a sustainable CO_2 sequestration process.

Table 1. The most commonly used API class well cement types (Developed after Robins & Milodowski, 1986).

API Class	Depth (m)	Temperature (°C)	Sulphate	Comments
A	0-1830	77	Ordinary	Regular cement
B	0-1830	77	Moderate	Regular cement
C	0-1830	77	Ordinary-High	High early strength
D	1830-3050	110	Moderate-High	For high pressure and temperature
E	1830-4270	143	Moderate-High	
F	3050-4880	160	Moderate-High	
G	0-2440	93	Moderate-High	OPC
H	0-2440	93	Moderate	OPC

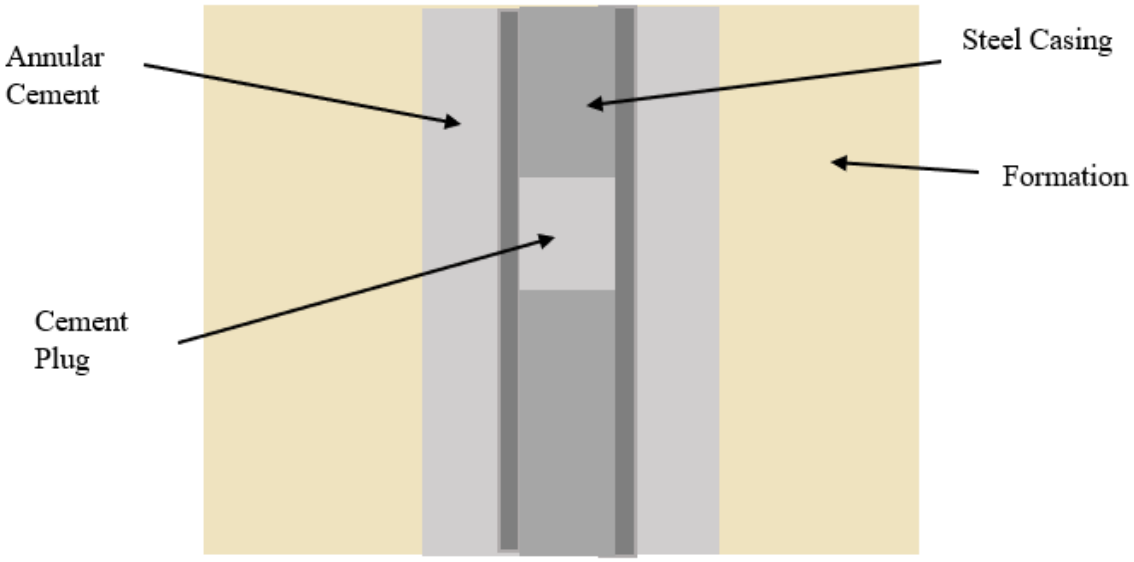

Figure. 4. A typical wellbore with primary and secondary cementing zones (Developed after Nasvi et al., 2013).

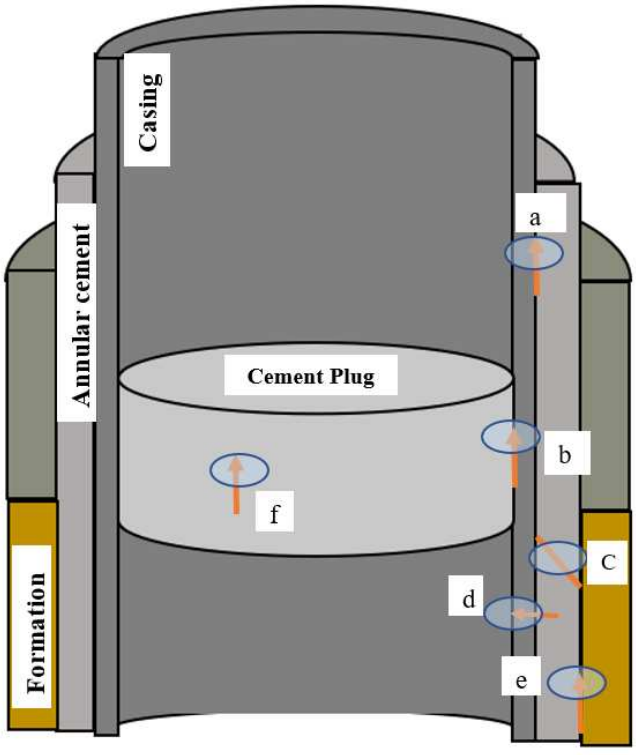

Figure. 5. Possible leakage pathways through the wellbore: (a) in the middle of cement and casing, (b) between cement plug and casing, (c) through the fracture of cement, (d) through the corroded casing, (e) between the formation and cement, and (f) through the pores of cement.

4. Ordinary Portland Cement (OPC) as a well cement and its problems

Researchers have done many experimental studies for identifying the behaviour of OPC-based well cement in an environment with a high concentration of CO_2. These experiments were mainly conducted using High Pressure and High Temperature (HPHT) vessels to maintain or simulate downhole conditions by controlling temperature and pressure gradients. These vessels usually consist of brine-saturated CO_2 and supercritical CO_2. These apparatuses were used to examine the carbonation of cement, the effect of the curing period, durability changes, and identify the mechanical behaviour of well cement in different states of CO_2 environment (Barlet-Gouédard et al., 2009). Some of the most pertinent literature on different types of OPC in various conditions and the key findings are summarised in Table 2.

The cement sheath in a well bore is the first material exposed to the injected CO_2 in the sub-surface during the sequestration process. Long-term CO_2 sequestration includes contact with supercritical CO_2 and brine solutions at increased pressure and temperature and decreased pH levels. When OPC-based well cement is exposed to CO_2-saturated brine under down-hole pressure and temperature conditions, a series of rings are observed, as shown in Figure 6 (Brandvoll et al., 2009; Duguid & Scherer, 2010). In fact, the different zones observed are: 1) an un-reacted dark grey core in the middle, 2) a grey layer with depleted $Ca(OH)_2$ (zone 1), 3) a white layer precipitated with $CaCO_3$ due to carbonation (zone 2), and 4) an orange layer with highly depleted $Ca(OH)_2$ and C-S-H paste (zone 3).

Generally, the carbonation of cement minimizes porosity and permeability under atmospheric conditions. However, under downhole conditions, OPC-based well cement reacts with dissolved CO_2 and is prominent to produce weak porous gel owing to the absence of a C-S-H layer, which causes an increase in the porosity and permeability of well cement (Kutchko et al., 2007). In addition, they are influenced by the degradation rate and degradation method of well cement in environments with high

concentrations of CO_2. As listed in Table 3, pressure and temperature variations, state of the fluid, type of fluid, cement composition, water-cement ratio, pH gradient, and mechanical loading are some of the influential factors that affect the integrity of the OPC-based well cement. As summarised in Table 3, the effects of the influential factors were studied by many researchers, and those observations are important to assess the performance of OPC-based well cement under downhole conditions. The problems about generally used OPC as a well cement that has been recognized in laboratory tests are experienced in practical situations as well. For instance, among the research done with 316,500 abandoned wells in Canada, 4.6% showed leakages, and of those leakages, 81% reportedly specified that OPC-based well cement is the main factor causing the leakages (Nasvi et al., 2014). Therefore, there is a requirement for finding a new well cement material to replace the generally used OPC under partial or full conditions, to carry out safe CO_2 sequestration processes.

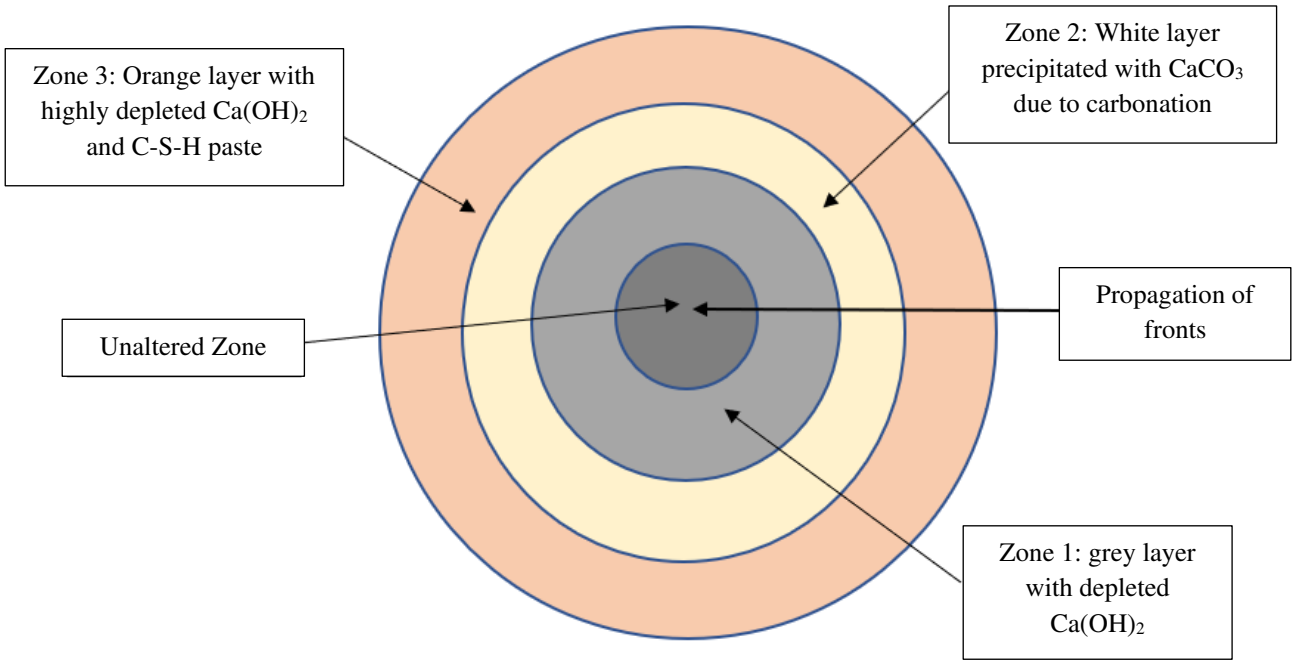

Figure. 6. Schematic view of different zones formed in OPC-based well cement in CO_2-rich environments (Developed after Duguid & Scherer, 2010).

Table 2. Previously reported key findings about different classes of OPC-based well cement.

Reference	Tested cement type	Experimental conditions				Findings
		State of CO_2 environment	Pressure	Temperature	Exposure Time	
Duguid & Scherer, 2010	Class H cement	CO_2-saturated brine (pH varied from 3 to 7)	-	50 °C	1, 2, 3, 6, and 12 months	Degradation of the grout was shown as 0.58 mm after 6 months. The rate of degradation of the cement was controlled by the rate of dissolution of the calcium carbonate-rich layer.
Condor & Asghari, 2009	Class A cement Class G cement	Wet supercritical CO_2 CO_2-saturated brine	15 MPa	55 °C	3 months	Permeability was reduced initially but increased after a few months. Compressive Strength was increased initially but reduced with the time.
Zhang & Talman, 2014	Class G cement	CO_2-saturated brine	10 MPa	53 °C	3, 7, 14, 28, and 84 days	The durability of the cement was decreased, and permeability was changed from 0.16 mD to 1.1 mD, at the final stage of the observation period.

Pratt et al., 2009	Portland cement	Wet supercritical CO_2	10 MPa	50 °C	84 days	A 200 µm carbonation depth was observed.
Santra et al., 2009	Cement + silica fumes + fly ash	CO_2-saturated water	14 MPa	93 °C	15 and 90 days	A 7 mm penetration depth was observed, and no improvement was observed when increasing the silica fumes.

1

2 **Table 3.** The effect of different factors on the behaviour of OPC-based well cement during the CO_2 sequestration process.

References	Influential factors	Cement class	Experimental conditions	Key findings	Conclusion
Laudet et al., 2011	Pressure and temperature	Class G	Pure class G cement was tested at 90 °C, and 35% of silica mixed class G cement was tested at 140 °C, where the samples were exposed to CO_2-saturated water at 8 MPa.	After 3 months, a 5 mm carbonation front was developed in the outer region at 90 °C and the propagation front reached the entire cross-section of 20 mm at 140 °C.	A higher rate of carbonation occurs at elevated temperatures.
Sauki & Irawan, 2010	Pressure and temperature	Class G	Tested under 10.5 MPa and 14 MPa pressures and 40 °C and 120 °C temperatures.	50% Ca depletion was observed at 10.5 MPa, whereas the reduction was only 2% at 14 MPa. 0.9 mm and 1.5 mm penetration depths were	The highest depth of penetration occurs at lower pressures and higher temperatures.

				observed at 40 °C and 120 °C of temperatures, respectively.	
Duguid & Scherer, 2010	State of fluid	Class H	Tested the effect of moving brine at room temperature and 50 °C of temperature.	Severe cement degradation (0.244 mm/day) was observed after 31 days, and total loss of portlandite [$Ca(OH)_2$] and calcium silicate hydrate (C-S-H) was observed in the outer regions.	Under moving brine conditions, the transport of reactants and reaction products by the forced advection enhances the chemical reaction, leading to severe degradation.
Brandvoll et al., 2009	State of fluid	Class G	Tested under both static CO_2-saturated water and moving fluid, and CO_2-brine system at 50 °C temperature and 10 MPa pressure.	The propagation of carbonates was limited to the surface during the static fluid condition (i.e., approx. 200 µm after 30 days), whereas extensive cement degradation (producing porous amorphous silica gel) was observed under the moving brine condition.	High degradation rate yields at the moving fluid condition.
Huerta et al., 2009	Mechanical loading	Class H	Subjected to the coupled effect of confining stress and acid treatment. The effect of the following on aperture size distribution was studied: cyclic loading and unloading; re-assembling of cores to study the new	An increase in confining pressure reduced the effective fracture aperture size and acid treatment altered the mechanical properties of the cement, and as a result, the fracture aperture was very narrow, (i.e., 10 µm at 3.5 MPa	Leakage paths through the cement can be self-healing under down-hole stress and acid exposure conditions.

			alignment of fractures; and acid treatment (HCl exposure of cement cores for 7-12 days).	confinement) compared to that of un-reacted samples.	
Huerta et al., 2009	Cement composition	Class H	Two cement mixtures were tested with pozzolan: cement ratio of 65:35 and 35:65, using fly ash as pozzolan and class H cement under sequestration environments (i.e., 50 °C temperature and 15 MPa pressure).	65:35 pozzolan blends had severe penetration rates (i.e., complete degradation within 2 days) compared to 35:65 blends (i.e., penetration depth is approximately 5 mm after 9 days)	Higher penetration rates occur at high pozzolan: cement ratios.

1

5. Fly ash (FA)-based geopolymers as an alternative well cement

The manufacturing process of OPC produces approximately 1.35 billion tons of greenhouse gases per year and it is estimated as 7% of the entire greenhouse gases which are emitted to the atmosphere annually (Hardjito et al., 2004). By considering this issue, geopolymers were introduced as a construction material to build high-quality infrastructures and used as an environmentally friendly material in the construction industry with the requirement of 50% less energy consumption in the manufacturing method due to the low process temperature procedure, as shown in Figure 7 (Hewayde et al., 2006). Not only environmental friendliness but also geopolymer has a cost-effective production method compared to OPC, as the cost of geopolymer production is normally 10%-30% less than that of OPC (Rangan, 2008). The raw materials of geopolymer include metakaolin, ground granulated blast furnace slag (GGBFS), fly ash, sedimentary and rock powder, silica fume, and alkali feldspars (Hardjito et al., 2004). Among them, worldwide fly ash production was estimated at around 780 million tons per annum. Generally, most of the ashes produced by burning coal in power plants are disposed of in landfills. These improper disposal methods create significant environmental and social problems due to the accumulation of heavy metal substances in the ground, causing the contamination of the groundwater table and damaging the surrounding flora and fauna. Therefore, the use of FA-based geopolymer for well cement has a higher prominence due to its ability to reduce the gigantic amounts of fly ash piled up due to coal-fired power plant operations (Ridha et al., 2018). On the other hand, in the production of 1 tonne of geopolymeric cement, only 0.184 tonnes of CO_2 is emitted, which is approximately one-sixth of the CO_2 amount produced during the manufacturing process of 1 tonne of OPC (Yang et al., 2009). Therefore, the above facts confirm the appropriateness of FA-based geopolymer for the replacement of OPC as an alternative well cement material for the CO_2 sequestration process, in the context of environmental and technical feasibility.

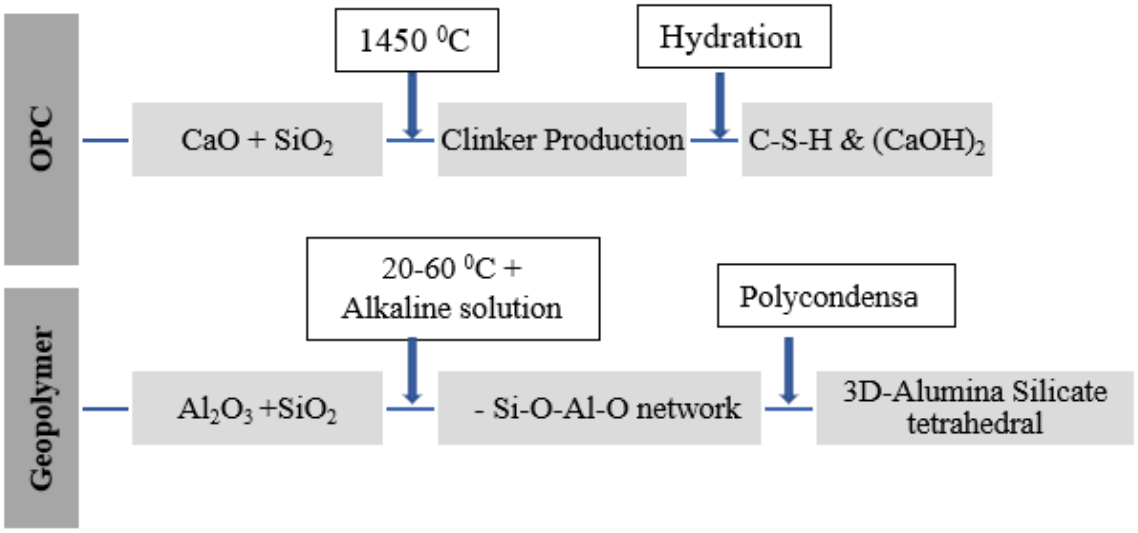

Figure. 7. Comparison between OPC and geopolymer productions (Developed after Hewayde et al., 2006).

With the introduction of FA-based geopolymer as a replacement for OPC as well cementing material, it was first researched by Davidovits (1994). Geopolymer is an alumino-silicate cementitious substance, which is activated by an alkaline solution with the combination of NaOH and Na_2SiO_3 (refer to Figure 8). The chemical formula of geopolymers can be generally expressed as in Eq. 1.

$$Mn[-(SiO_2)z - AlO_2]n.wH_2O \quad (1)$$

Where, M is the alkaline element such as Potassium, Sodium, or Calcium; n refers to the amount of polycondensation or polymerization and z is the ratio of Si/Al, that is 1, 2, 3, or higher (Nasvi et al., 2013).

The alumino-silicate source substances can be synthetic pozzolanas or Alumina Silicate-based industrial by-products, or a mixture of these.

Figure. 8. The schematic view of Geopolymer preparation.

From previous studies, it is found that FA-based geopolymer demonstrates better performance under wellbore conditions compared to the OPC in terms of several properties including high strength, low permeability, high pump-ability, long-term durability, high sulphate resistance, high volume stability, high thermal stability, less creeping action, less drying shrinkage, high surface smoothness and high resistance to acidity (Khalifeh et al., 2014). As listed in Table 4, the chemical compositions of OPC and FA mainly affect their respective properties and the consequent mechanical behaviour.

Table 4. Chemical analysis of OPC and class F fly ash (Developed after Sagoe–Crentsil et al., 2010).

Chemical element	OPC (wt %)	Fly Ash (wt %)
SiO_2	20.20	47.19
Al_2O_3	4.16	29.79
Fe_2O_3	5.30	13.93
CaO	64.80	3.29
MgO	1.29	1.38
Na_2O	0.22	0.24
K_2O	0.42	0.49
TiO_2	-	1.77
SO_3	2.67	0.13
LOI	1.34	1.3

Experimental studies were conducted to identify some specific properties of the FA-based geopolymer and OPC, which give a comparative idea between OPC and FA-based geopolymer. In fact, FA class C and OPC class H were examined under different test procedures by Ahdaya & Imqam (2019). Their stability test results proved the inability of OPC to hold the water, as it showed a loss of water percentage of 2.28%. However, the tested FA-based geopolymer did not give any loss of

water during the observed period. The sedimentation test, which was one of the stability tests showed the difference in density between FA-based geopolymer and OPC with time, which were 0.008 g/cm^3 and 0.028 g/cm^3, respectively. This specifies that there is no considerable particle sedimentation occurred in the FA-based geopolymer during the observed time period. However, the selected class C geopolymer and class H cement exhibited the same rheological behaviour (Ahdaya & Imqam, 2019). Especially in downhole conditions, OPC generally forms $CaCO_3$ under CO_2 rich environment and causes a pH drop from 12-13 to 7-8. This in turn causes the degradation of the OPC applied between casing and caprock interfaces (Nasvi et al., 2012b). In the case of FA-based geopolymer, it was found that Na_2CO_3 or K_2CO_3 with a pH of approximately 10 delivers high resistance to degradation under an acid-rich environment (Davidovits, 2005). Further, OPC and geopolymer were tested by Uehara (2010) in different acidic environmental conditions, where OPC failures were observed after 4 months in a 10% H_2SO_4 experimental condition. Since OPC minerals reacted with an acidic solution, a high degradation of the OPC sample occurred because of its inability to withstand acidic surroundings. In contrast, FA-based geopolymer did not show significant changes in its microstructure, and appeared to be showing high compressive strength values, compared to that of OPC (Uehara, 2010).

From the preliminary review, it is found the FA-based geopolymer demonstrates a better performance over OPC as a well cement for the CO_2 sequestration process. The following sub-sections comprehensively discuss the characteristics of FA-based geopolymer and its superior performance in different aspects as a well cement over conventional OPC-based well cement.

5.1. The role of chemical characteristics of FA in FA-based geopolymer

The chemical characteristics of the FA-based geopolymer used as the well cement significantly depend on the chemical composition of the particular FA used for the production – as FA is the major

component of the geopolymer. Therefore, it is essential to thoroughly study the chemical composition of the FA used for the geopolymer, before using it on an industrial scale.

The chemical composition of FA is controlled by the source of the coal, the type of furnace, the operating conditions, and post-combustion parameters (Kutchko & Kim, 2006). The chemical composition of FA was analysed either by X-Ray Fluorescence (XRF) or X-Ray Diffraction (XRD) analyses. In general, the chemical composition of FA is very similar to that of bottom ash. FA is primarily composed of Silica (SiO_2), Ferric Oxide (Fe_2O_3), and Alumina (Al_2O_3), with smaller quantities of Calcium Oxide (CaO), Sodium Oxide (Na_2O), and Sulphur Trioxide (SO_3). In fact, the Calcium Oxide (CaO) percentage decides the fly ash category, where the fly ash with higher than 20% of CaO is referred to as Class C, whereas lower-calcium fly ash is classified as Class F (Nasvi et al., 2013). The chemical configuration of the fly ash class is highly important for the geo-polymerization process, as it decides the characteristics and microstructure of the final product (refer to Table 5). By considering these effects, class F FA is mostly used for FA-based geopolymer cement (Nasvi et al., 2013).

Table 5. Chemical composition (%) of Class F fly ash and Class C fly ash (Developed after Guo et al., 2010).

Element		**SiO_2**	**Al_2O_3**	**Fe_2O_3**	**MgO**	**CaO**	**SO_3**	**K_2O**	**Na_2O**	**LOI**
Composition	Class F	50.0	28.0	12.0	0.6	6.5	-	1.5	0.2	-
	Class C	38.0	19.0	9.0	5.0	20.0	3.0	0.4	1.0	3.5

The chemical composition of FA in different countries that were collected from the literature is graphically represented in Figure 9. A detailed summary including the country, generated power plant, and the chemical composition of the FA are given in Annex A. In fact, the chemical properties

of FA play an important role in the utilization of FA, as they may cause some adverse environmental impacts, such as trace metal contamination in the groundwater, health hazards to living beings, and loss of fertility in the soil (Fulekar & Dave, 1986). Therefore, it is essential to conduct a chemical analysis to assess whether it contains any constituents that are harmful to the environment and its living beings, before utilizing them for producing FA-based geopolymers.

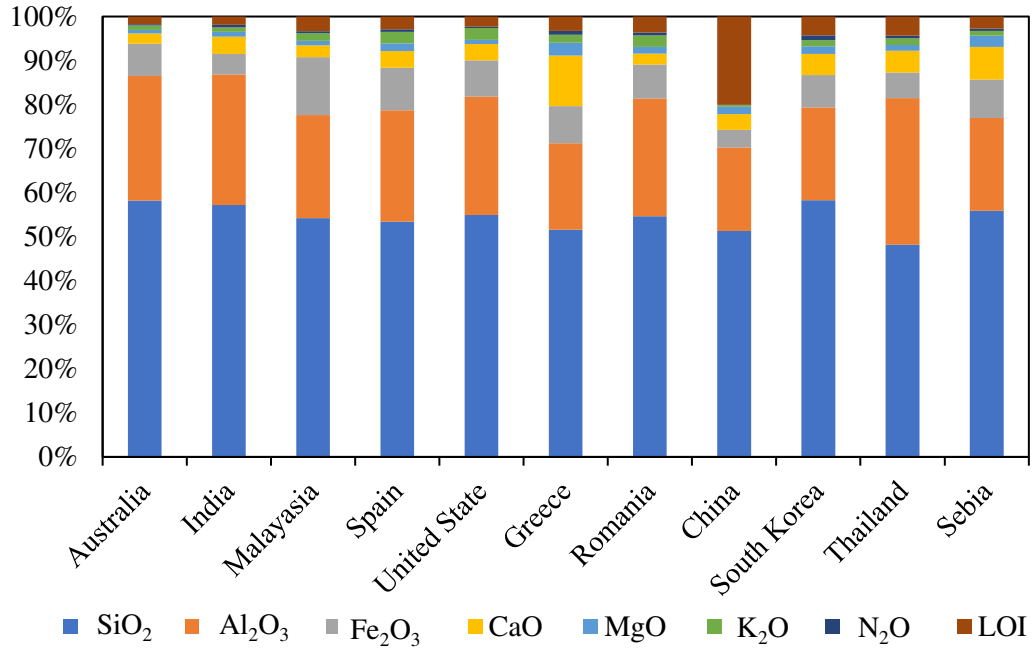

Figure. 9. Variation in the chemical composition of FA in different countries.

5.2. The role of alkaline activator and other elements in FA-based geopolymer

The source materials are activated by alkali to take part in the geo-polymerization process and reacted with Si and Al to make a geopolymer binder (Ridha et al., 2018). The alkali activator is generally an alkali hydroxide or alkali silicate solution such as Sodium Silicate (Na_2SiO_3), Sodium Hydroxide (NaOH), Sodium Carbonate (Na_2CO_3), Potassium Carbonate (K_2CO_3), Potassium Hydroxide (KOH), water, and some mixtures of these (Nasvi et al., 2013). The most common activators are NaOH and Na_2SiO_3 due to their availability, economic feasibility, and efficiency. As a result of a combination

of Na_2SiO_3 and NaOH, it creates a solid substance with fewer apertures and provides a sturdy connection between the geopolymer matrix and the aggregate. A high percentage of NaOH concentration involves leaching the Si and Al ions in NaOH solution, which is directly influenced to generate higher compressive strength (Ahdaya & Imqam, 2019). Therefore, the chemical concentration and the ratios, which are mixed in geopolymer, are directly involved in deciding the properties of the final FA-based geopolymer cement. Due to that effect, researchers have done experimental work on identifying the variation of geopolymer characteristics with the changes in content ratios of chemical elements. In fact, many research works have shown the effect of changing several physical properties with the variation of the 1) alkaline activator to fly ash ratio, 2) Sodium Silicate to Sodium Hydroxide ratio, and 3) Sodium Hydroxide concentration.

Figure 10, developed after Ahdaya & Imqam (2019) shows the variation of physical properties of class C FA-based geopolymer paste including density, compressive strength, and fluid loss under different chemical ratios. Further, Hardjito et al. (2008) tested both class C and class F fly ash by increasing the alkaline activator to fly ash ratio and observed an increment in the compressive strength, in which 0.40 of optimum activator to fly ash ratio yielded the highest compressive strength (refer to Figure 11). In addition, the influence of mixed composition on compressive strength was deeply examined by Thakur & Ghosh (2009) using different percentages of alkali content and silica content. In this case, compressive strength of class F FA-based geopolymer with different alkali percentages of 0.46%, 0.50%, 0.54%, 0.58%, 0.62% was tested in 3 days, 7 days, and 28 days, where the test results showed a linear increment with increasing alkali content (refer to Figure 12). The highest compressive strength of 48.20 MPa was observed for maximum alkali content (Na_2O/Al_2O_3) of 0.62. (Thakur & Ghosh, 2009) also examined the silica content (SiO_2/Al_2O_3) *vs.* compressive strength using different silica contents, such as 3.70%, 3.85%, 4.00%, 4.15%, 4.30% (refer to Figure 13). Noticeably, it has shown a similar behaviour as in Figure 11, where the compressive strength variation showed a slight increment, yielding an optimum compressive strength at a silica content of approximately 4.15%, beyond which the compressive strength reduces with the increasing silica

percentage. In addition to the above characteristics, the physical appearance at the elevated temperature also depends on the Si/Al ratio of the FA-based geopolymer mixture (Thokchom et al., 2012).

Tested Property	Method	Observations
Compressive Strength	Increased the NaOH concentration from 5M to 10M under constant Na_2SiO_3 to NaOH ratio of 0.25	Compressive strength increased from 5.59 to 8.52 MPa
Density	Changed the alkaline activator to fly ash ratio from 0.2 to 0.4 with NaOH concentration of 10M	Density of FAG was decreased when alkaline activator to FA ratios increase
Fluid Loss	Changed the alkaline activator to fly ash ratio from 0.2 to 0.4 with NaOH concentration of 10M	Fluid loss volume was changed from 7.33 to 3.1 ml/min

Figure. 10. Variation of physical properties with the changes in chemical concentration of fly ash class C (Developed after Ahdaya & Imqam, 2019).

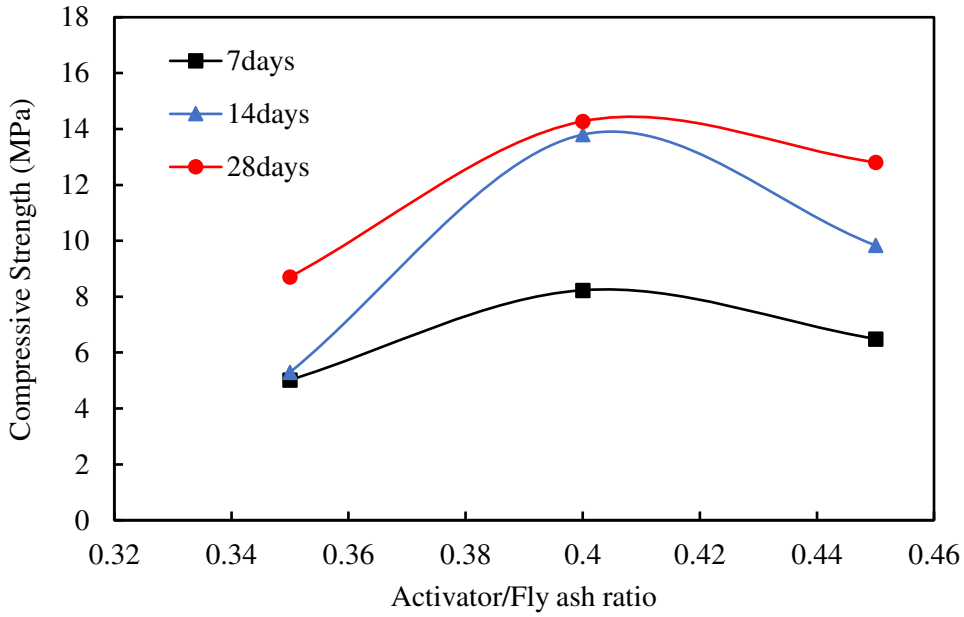

Figure. 11. Variation of Compressive strength with the different alkaline activator to fly ash ratio (Developed after Hardjito et al., 2008).

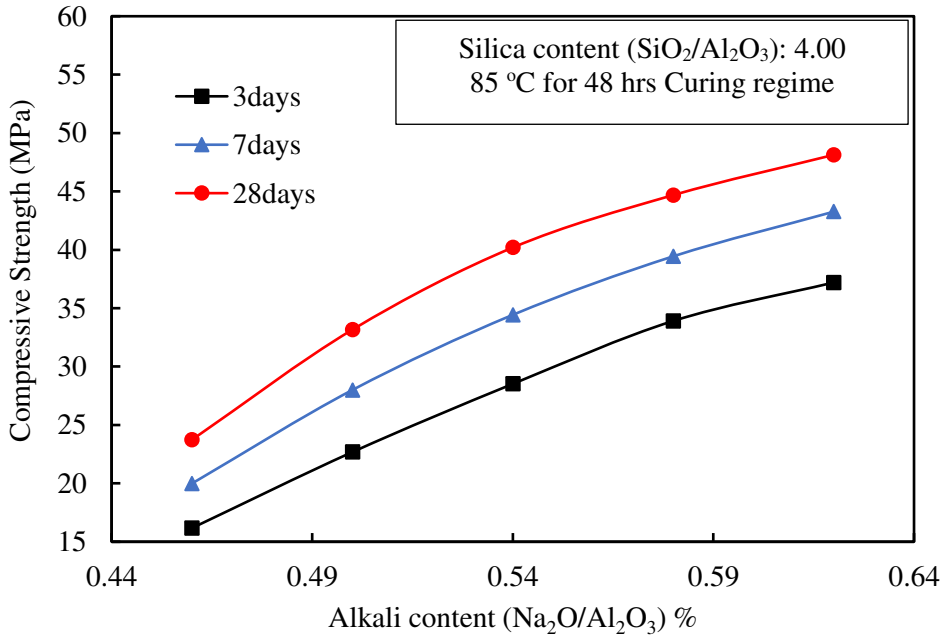

Figure. 12. Variation of Compressive strength with the different alkali contents (Developed after Thakur & Ghosh, 2009).

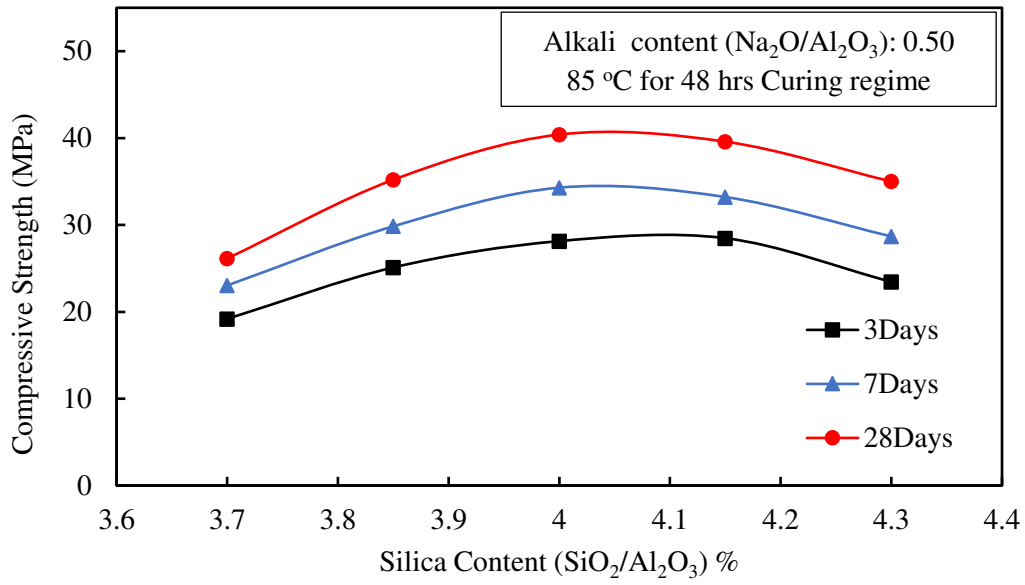

Figure. 13. Variation of Compressive strength with the different silica contents (Developed after Thakur & Ghosh, 2009).

Further, the cracks that appeared in the microstructure of FA-based geopolymer well cement was investigated by researchers under different elevated temperatures, where the microstructure effects have been scanned by using Scanning Electron Microscopy (SEM) and Energy Dispersive X-ray (EDX) tests. Geopolymer cement with a higher Si/Al ratio shows lesser crack formation, comparatively to the mixtures with lesser Si/Al ratios (Thokchom et al., 2012). These results were obtained by using the geopolymer samples with Si/Al ratios of 1.9, 2.2, and 1.7, under three main elevated temperatures of 300 °C, 600 °C, and 900 °C. According to the X-ray diffractogram, geopolymers with 1.7 and 2.2 of Si/Al ratios showed different behaviour under exposure to 900 °C. As a result, the geopolymer with a low Si/Al ratio of 1.7 has given a highly amorphous nature and showed less amorphous phases in the geopolymers with a high Si/Al ratio of 2.2. According to these experimental results, it was confirmed that FA-based geopolymers with high Si/Al ratios have shown high stability under elevated temperatures (Thokchom et al., 2012).

Especially, at downhole conditions, the temperature gradient is assumed to be 30 °C/km, which can be varied with the location (Nasvi et al., 2012a). The well cement which is used in the CO_2 sequestration process should have a greater stability and a crack-free surface to carry out a successful CO_2 sequestration process under elevated temperatures and high pressures. Therefore, it is highly important to carefully determine the correct elemental compositions of FA-based geopolymer mixture to produce a well cement that would be stable under downhole conditions.

5.3. The role of curing conditions in the mechanical aspects of FA-based geopolymer

The depth of the injection wells which are used in the CO_2 sequestration process can vary from 0.8-2 km and the temperature can vary from 30 °C to 80 °C at the deepest location of the well with a pressure variation up to 50 MPa (Nasvi et al., 2012b). In most cases, curing conditions such as curing temperature, curing time, and categories of curing support to predict the performance of geopolymer at downhole conditions (Nasvi et al., 2013). Numerous experimental studies were done to investigate the compressive strength, Poison's ratio, stress-strain changes, and crack initiation at altered curing temperatures. Heat is a major accelerator for the geo-polymerization process, due to which, the curing was normally carried out at elevated temperatures. According to past studies, it was revealed that by increasing the curing temperature up to 60 °C, geopolymer cement achieves up to 70% of its strength in the first 4 hrs of setting time, where the setting time and curing temperature show an inverse relationship (Nasvi et al., 2013). When the temperature was raised from 30 °C to 50 °C to 75 °C, the Al and Si precursors were highly dissolved from the source material and the related setting time was reduced (Tempest et al., 2009). Since high pressure and temperature are used in general CO_2 sequestration wells, reduced setting time is possible under wellbore conditions, and this has to be adjusted to achieve a workable mix to fill the annular surface and allow sufficient time before hardening. According to the practical circumstances, FA-based geopolymer cement can be handled for a period of up to 2 hrs without any setting, in the cured temperature range of 65 °C to 80 °C

(Hardjito et al., 2008). In general, the nature of the downhole conditions requires 1 to 4 hrs setting time, according to the temperature and the pumping rate of the cement slurry. Therefore, investigations have been conducted to observe the suitability of retarders for the geopolymers to improve the setting time (Nasvi et al., 2013).

Curing time is also an important aspect that affects the characteristics of FA-based geopolymer well cement. Many works done in this aspect have shown that the increase in curing time tends to increase compressive strength. However, there is no substantial increase observed after 48 hrs (Thakur & Ghosh, 2009). In fact, class F FA-based geopolymer samples have been tested with alkali and silicate contents, and water-to-geopolymer solid ratios of 0.62, 4.0, and 0.228, respectively. These specimens were placed in an oven under air pressure and temperature at 85 °C for a variable duration of 4 to 72 hrs. The highest compressive strength of 40.8 MPa was obtained with 48 hrs of curing time, but the rise of curing time did not affect the increase of compressive strength further (Thakur & Ghosh, 2009). This confirms that geopolymer attains its ultimate compressive strength in a short period of curing time with a significantly high geo-ploymerization process (Hardjito et al., 2004). However, it is found that quick curing at higher temperatures would produce cracks, which makes a negative impact on the characteristics of geopolymer cement. On the other hand, the compressive strength has shown a significant reduction when cured at a higher temperature for a longer period, as this breakdowns the granular structure of the geopolymer mixture (Hardjito et al., 2004).

In fact, the impact of curing temperature was studied by Hardjito et al. (2004) using specimens with 0.62 of alkali content and 4.0 of silica content. These samples were cured for 48 hrs changing the curing temperature from 45 °C to 120 °C under atmospheric pressure. The maximum compressive strength of 48.2 MPa was obtained at the optimum temperature of 85 °C. Nasvi et al. (2015) investigated the mechanical behaviour of geopolymers at various curing temperatures from 20 °C to 80 °C, under triaxial experimental conditions. Their experimental result also confirmed the above observations by getting the deviatoric strength increment from 20 MPa to 105 MPa, when increasing the curing temperature from 23 °C to 60 °C, and showed a 15% of deviatoric reduction with the rapid

change of curing temperatures from 60 °C to 80 °C (Nasvi et al., 2015). As illustrated in Figure 14, beyond 60 °C, the strength level is closer to the stabilized level, which does not give further strength increment with the curing temperature.

Not only compressive strength but also stress-strain behaviour and crack occurrence also depend on curing temperature. In fact, the tested samples have shown higher strains of approximately 6-8% at failures, at lower temperatures such as 23 °C and 30 °C, whereas high-temperature cured samples (i.e., cured at 40 °C to 80 °C temperature) have experienced low strains of approximately 0.8-3.5% at failure. These results conveyed that the FA-based geopolymer well cement may have behaved as a brittle material at high temperatures (Nasvi et al., 2012b).

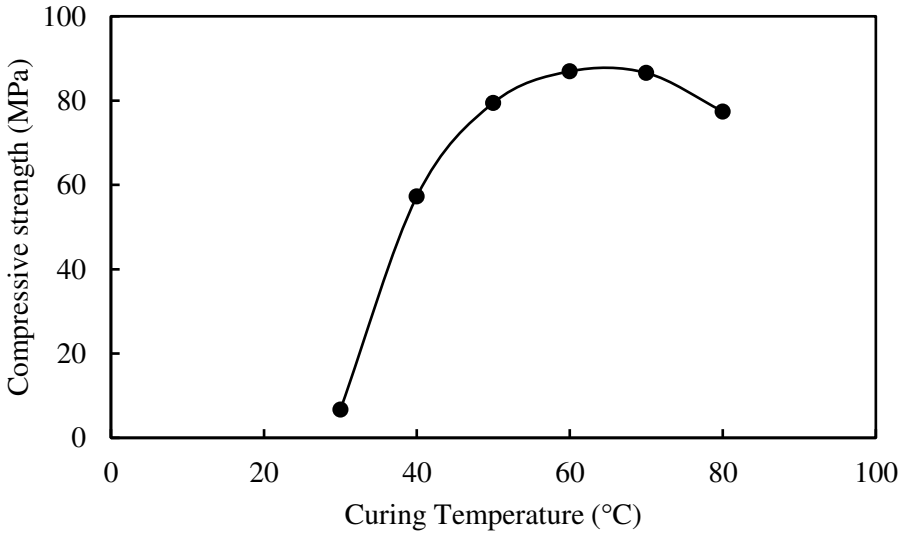

Figure. 14. Variation of compressive strength of geopolymer well cement with curing temperature (Developed after Nasvi et al., 2015).

The curing environment was examined by Sagoe–Crentsil et al. (2010) to identify the effect on compressive strength by using OPC and class F FA-based geopolymer samples, during which two curing environments were used, i.e., 1) heat curing and 2) ambient curing (refer to Table 6). According to the results, A relatively speedy early strength gain was shown by OPC samples

compared to geopolymer samples at ambient curing environment. These results showed that ambient temperature can also make an influence on the rate of early strength increment (Sagoe–Crentsil et al., 2010).

It is evident from the above studies that curing condition has a significant effect on the performance of FA-based geopolymer; thus, needs to be controlled cautiously to achieve the required level of performance.

Table 6. Compressive strength development for ambient and steam curing conditions (Developed after Sagoe–Crentsil et al., 2010).

Compressive strength	OPC		Class F FA-based geopolymer	
	Steam curing environment (MPa)	Ambient curing environment (MPa)	Steam curing environment (MPa)	Ambient curing environment (MPa)
1 day	22.50	9.10	42.30	-
3 days	-	-	-	2.00
7 days	28.00	35.40	42.30	7.20
28 days	38.10	43.70	44.00	35.50

5.4. The role of elevated temperature on the behaviour of FA-based geopolymer cement

Different studies were conducted to identify the surface evaporation effect using sealed and unsealed conditions during the curing process and the strength variation of different FA-based geopolymer pastes in different elevated temperature exposure conditions (Kannangara et al., 2021). These experimental results concluded that less excess initial surface evaporation can occur with high strength values for sealed geopolymer specimens under elevated temperatures. Unsealed geopolymer samples have shown approximately 35% and 25% lesser values for the residual strength results at 400 °C and 800 °C, respectively, where they have caused a higher degree of thermal cracking and

splitting compared to the sealed geopolymer samples (Kannangara et al., 2021). Experimental works have been conducted to study the comparative behaviour of geopolymers made with metakaolin and FA after exposure to elevated temperatures. The FA-based geopolymer has shown an increment in strength after exposure to elevated temperatures (i.e., 800 °C), while metakaolin-based geopolymer has shown a reduction in strength after similar exposure. The availability of a large number of small pores on FA-based geopolymer cement is the reason for the observed result, where these pores facilitate the escape of moisture when heated, triggering minimal damage to the geopolymer matrix (Kong et al., 2007). Although FA-based geopolymer did not show any noticeable cracks on the surface of the specimens after exposure to elevated temperature, metakaolin geopolymer has shown macro-cracks with widths of 0.1 to 0.2 mm due to the absence of pore distribution structures similar to the FA-based geopolymer (Kong et al., 2007). Ridha et al. (2020) showed that the crystal-like shape identified as calcium carbonate was formed at the surface of spherical fly ash particles after CO_2 interaction-induced carbonation. Although, the carbonation process occurred, no strength reduction was observed during the study. Further, microstructure analysis has discovered that zeolite has been formed during CO_2 acid exposure for geopolymer cement, which causes a slight development of strength. According to the above findings, FA-based geopolymers have shown to be suitable for well cement in CO_2 injection wells under elevated temperature conditions.

5.5. Hydro-mechanical behaviour of FA-based geopolymer well cement

5.5.1. Compressive strength and tensile strength of FA-based geopolymer

Compressive strength is one of the key characteristics that have a great influence on wellbore integrity at higher pressure conditions to ensure the structural support for the casing and hydraulic/mechanical isolation in the downhole environment (Di Lullo & Rae, 2000). Investigations on class G cement have concluded that conventional OPC is not capable of bearing the stress created by frequent pressure and temperature changes in wellbores (Pedersen et al., 2006). Researchers have experienced that the

performance of OPC-based wells dropped after 15 years when the wells were exposed to 180 ºC and 22% CO_2, and it was noticed that CO_2 is the main reason for degradation. In addition, it was concluded that higher temperature and CO_2 are the causes of the loss of compressive strength and cement integrity in the wells (Krilov et al., 2000). Figure 15 shows the compressive strength reduction of Class G (G) and Class A (Type T10) well cements in a CO_2 environment under 2200 psi and 55 °C pressure and temperature conditions. It is noticeable that the compressive strength of both class G and class A well cement reduces gradually with time, confirming the adverse impact imposed by CO_2 on conventional well cement (Condor & Asghari, 2009).

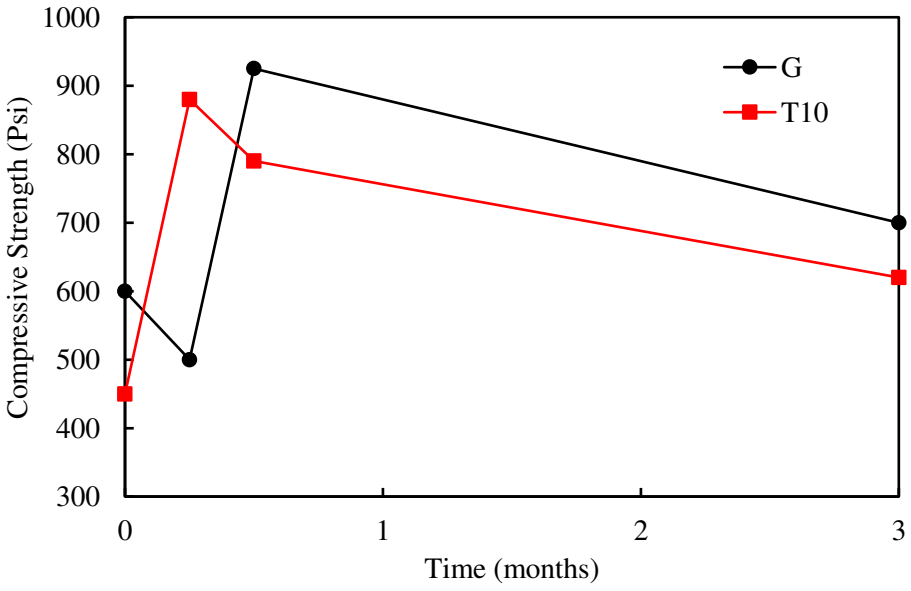

Figure. 15. Compressive strength variation of class G (G) and Class A (T10) well cements in CO_2 environment (Developed after Condor & Asghari, 2009).

The durability of class G well cement was investigated by Lécolier et al. (2007)**,** where class G cement samples were cured at 80 °C for one month, and samples were aged in water, brine, and crude oil at 80 °C. It was observed that samples aged in water and crude oil did not show considerable strength reduction after one year, whereas the uniaxial compressive strength (UCS) of the samples aged in

brine fell to 50% of the initial strength. These results concluded that the mechanical strength of OPC-based cement reduces in CO_2- rich downhole conditions due to cement degradation.

Not only compressive strength, but also tensile strength of well cement plays a vital role in cement integrity due to the following reasons: 1) if there are sufficient induced stresses to cause a mechanical failure of a set cement sheath, failure is probably of tensile nature (Goodwin, 1997), and 2) if the formation gas enters the cement pores and the gas pressure exceeds the tensile strength value of cement, a fracture is created leading to gas migration problems (Backe et al., 1999). Therefore, cement with higher tensile strength and higher tensile strength to Young's modulus ratio is preferred for well cementing (Mavroudis, 2001). In fact, the tensile strength of carefully mixed OPC-based well cement under API-recommended formulations varies from 1-2 MPa (Labibzadeh, 2010).

The tensile strength of geopolymer needs to be studied to predict its suitability as well sealant material. Many researchers have studied the tensile strength of alkali-activated geopolymer materials (Hardjito & Rangan, 2005; Raijiwala et al., 2012; Sakulich et al., 2009; Sarker, 2011; Sofi et al., 2007). A summary of their test methods and their salient findings are shown in Table 7, including the source material and test variables employed, the UCS, uniaxial tensile strength (UTS), and the ratio of UTS/UCS.

Table 7. A summary of previous studies related to compressive strength and tensile strength of geopolymers.

Reference	Source material, Test Variables	UCS (MPa)	UTS (MPa)	UCS/UTS (%)
Hardjito & Rangan, 2005	FA, different NaOH molarity and curing temperatures	44-89	4.4-7.4	8.3-10

Mishra et al., 2008	FA, different NaOH molarity values	13-27	0.9-3.1	5.6-9
Sofi et al., 2007	different FA types, H_2O/ FA ratio and slag content	47-57	2.8-4.1	5.2-8.3
Olivia & Nikraz, 2011	different activator/FA ratio and superplasticizer contents	56-60	4-4.3	7-7.3
Raijiwala et al., 2012	FA, different curing temperatures	39-55	4.1-6.5	10.5-11.7

Table 7 indicates that the tensile strength values range from 5.2-11.7% of the compressive strength, and the values vary significantly with the geopolymer mix compositions and test conditions used. The relationship between tensile and compressive strength depends on many factors such as age, strength of concrete, liquid/solid ratio, curing temperature, and type of curing (Zain et al., 2002).

Sarker (2011) compared the splitting tensile strength of FA-based-geopolymers and OPC based on their results and the findings from the literature. It was noticed that, for a given compressive strength, the splitting tensile strength of FA-based geopolymer is higher than that of OPC (refer to Figure 16). The higher tensile strength is attributed to the use of soluble silicates in geopolymers, where the soluble silicates produce denser interfacial transition zones between the aggregate and the cement matrix, leading to higher tensile strength values (Sarker, 2011).

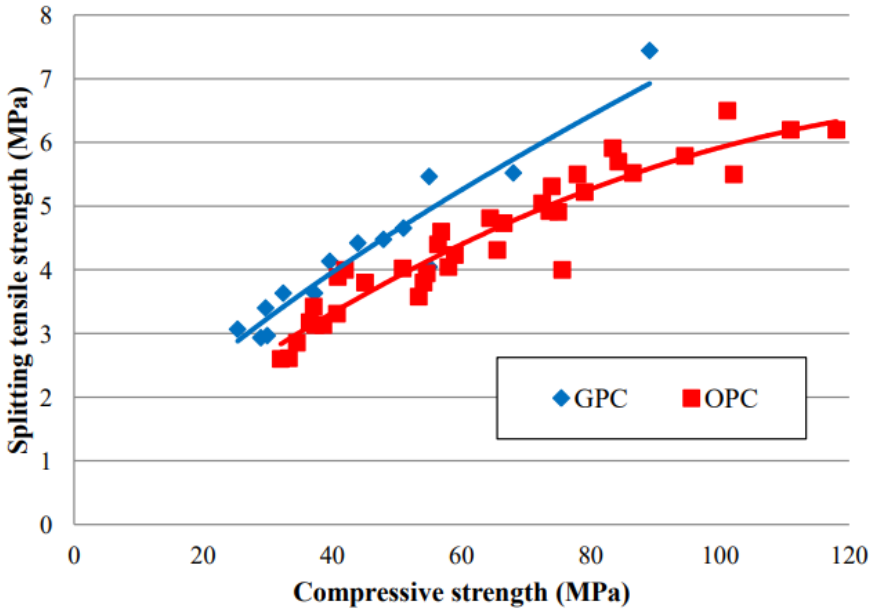

Figure. 16. Comparison of splitting tensile strength and the compressive strength of OPC and FA-based geopolymer well cements (GPC) (Developed after Sarker, 2011).

5.5.2. Permeability of FA-based geopolymer

The permeability of the well cement is the major problem compared to strength-related problems. The low permeability is the main indicator that promotes the leakage-free nature of the sequestration process (Nasvi et al., 2014). Especially at downhole conditions, the generally used OPC was degraded due to the CO_2-rich environment, causing the increment in permeability and porosity (Nasvi et al., 2014). The permeability of FA-based geopolymer well cement was tested under different mix compositions to recognize the effect of the chemical mixture on the permeability variation. An experiment was done by Van den Heede et al. (2010) to check the Oxygen permeability using four different FA-mixed samples, which included 0%, 35%, 50%, and 67% of FA amounts. The test results showed low permeability values of 0.5-2.0 $\times$ 10^{-16} m^2 for most of the FA-containing samples, compared to generally used OPC samples with a 3.0 $\times$ 10^{-16} m^2 permeability. These findings indicate that the pores in FA-containing samples are less connected due to the additional hydration products created by the pozzolanic FA reaction, causing the low permeability. Not only the FA composition

but also researchers have investigated the permeability of FA-based geopolymers by adding different slag amounts and compared the permeability values with class G cement, under CO_2 environments (Nasvi et al., 2014). The test samples were made by partially replacing FA with alkali-activated slag in 0%, 8%, and 15% by mass. The CO_2 permeability of these samples has been varied from 0.002-0.019 µD, 0.002-0.021 µD, and 0.0005-0.002 µD, respectively. The outcomes of this study concluded that the permeability of geopolymer without alkali-activated slag and the geopolymer with 8% slag is 100 times lower than that of class G cement, where the slag with 15% mixture has given the lowest permeability which is nearly 1000 times lower than the permeability of class G cement in general. This is mainly attributed to the improvement of the microstructure of geopolymer with the addition of slag (Nasvi et al., 2014).

In typical downhole conditions, the well cement is exposed to a temperature range of 20-80 °C with a depth variation of 1.5 to 2 km. Therefore, the permeability variation under different temperatures was also examined by many researchers. An experimental study conducted by Nasvi et al. (2014) reported that the permeability values of FA-based geopolymer well cement increase with the increment in temperature for a given inlet and confining pressure. The most important finding is that the highest permeability value of geopolymer is nearly 5000 times lower than the recommended limit of 200 µD for well cement by the American Petroleum Industry (API). In addition to the above findings, a summary of the permeability values between OPC and FA-based geopolymer is shown in Table 8. In the case of conducting a successful CO_2 sequestration project, the idea about the permeability variation of well cement should be focused on; however, only limited studies have been conducted on testing the CO_2 permeability of fly ash-based geopolymers up to date.

Table 8. Previously reported permeability values for FA-based geopolymer and OPC-based well cement.

Reference	Permeating fluid	Permeability	
		Geopolymer	OPC
Van den Heede et al., 2010	Oxygen	3.0×10^{-16} m^2	$0.5\text{-}2.0 \times 10^{-16}$ m^2
Zhang & Talman, 2014	Water	$0.5\text{-}1.5 \times 10^{-12}$ m^2	1.0×10^{-10} m^2
Sagoe–Crentsil et al., 2010	Oxygen	6.19×10^{-17} m^2	6.32×10^{-17} m^2
	Water	1.52×10^{-10} m/s	1.73×10^{-11} m/s

5.5.2.1. Available models for predicting the CO_2 permeability of FA-based geopolymer

Some different empirical equations and models were developed by researchers to estimate the permeability of different liquids, materials, and gases. Some of these models have been tested to identify their applicability in the prediction of CO_2 permeability in FA-based geopolymer. Studies have been performed using the pressure transient approach to measure the permeability of brittle materials. In the pressure transient method, the boundary condition shown in Eq.2 has been used to calculate the flow rate through the sample (Siriwardane et al., 2009).

$$\frac{\partial p(L,t)}{\partial t} = \frac{Q}{\beta V} \tag{2}$$

Where p is the pressure, L is the length of the sample, t is the time, Q is the flow rate through the sample, V is the downstream volume, and β is the adiabatic compressibility of the gas.

The Hagen–Poiseuille expression (refer to Eq.3) can be used to calculate the permeability of a porous solid body for a compressible fluid. This equation assumes a linear variation between the volumetric flow rate and pressure gradient (Ranjith & Perera, 2011).

$$k_A = \frac{2Q\mu L p_{out}}{A({p_i}^2 - {p_{out}}^2)} \quad (3)$$

Where k_A is apparent gas permeability, μ is the fluid viscosity, L is the length of the sample, A is the area, Q is the flow rate, p_i and p_{out} are upstream and downstream pressures, respectively.

According to the experimental work that was conducted under drained conditions, a linear relationship has been derived to estimate the variation of CO_2 flow rate with injection pressures under different confining pressures (refer to Eq.4). Therefore, Eq.4 can be used to find the CO_2 permeability through FA-based geopolymer (Nasvi et al., 2013).

$$Q = -0.000417\, p_c + 0.00165\, p_{in} + 0.00484 \quad (4)$$

Where Q is the CO_2 flow rate (l/h), p_c is the confining pressure (MPa), and p_{in} is the injection pressure (MPa).

REFPROP database was used by Huber et al. (2008) to derive the viscosity (μ) and adiabatic compressibility (β) of CO_2 used in Eq.2 and 3 to develop a model regarding CO_2 permeability in a solid body. The REFPROP program, developed by the National Institute of Standards and Technology (NIST), provides information about the thermodynamic and transport properties of industrially important fluids and mixtures. The viscosity and adiabatic compressibility values of CO_2 taken from the REFPROP database for different mean pressure (P_m) and temperature (T) conditions are utilized in the test to identify the behaviour. Results showed a closer relationship between viscosity and adiabatic compressibility with pressure than temperature. In the subcritical pressure conditions (P < 7.2 MPa) the viscosity and adiabatic compressibility has not shown a significant variation with the temperature, whereas in the supercritical CO_2 conditions (P > 7.2 MPa and T >

31.8 °C), the variation of viscosity and compressibility has shown a considerable variation with both pressure and temperature.

In the case of developing the equations to predict the permeability of FA-based geopolymers at different temperatures under different confining pressures, the formula that was developed by Gawin et al. (1999) is widely used. This formula predicts the permeability of concrete at different temperatures and different gas pressure conditions using a mechanistic approach (refer to Eq. 5).

$$k_A = k_0 10^{A_T(T-T_0)} \left(\frac{P_g}{P_0}\right)^{A_p} \quad (5)$$

Where k_0 is intrinsic permeability at the reference temperature ($T_0 = 293\ K$), P_g is gas pressure, P_0 is atmospheric pressure, and A_T and A_p are material-dependant constants.

The above formula (refer to Eq. 5) has been used to predict permeability under drained conditions, where the downstream pressure is always 0.1 MPa. Since the downhole pressure is not constant in actual scenarios, Nasvi et al. (2014) performed an undrained triaxial experiment to improve Eq.5. Through that, they developed a formula for downstream pressure using regression techniques as shown in Eq. 6.

$$P_{out} = A\left(\frac{T-T_0}{T+T_0}\right) + B\left(\frac{P_{in}}{P_c}\right) - C \quad (6)$$

Where T_0 is the reference temperature (K), P_{in} is the inlet pressure (MPa), P_c is the confining pressure (MPa), A and B are material constants depending on the temperature and mechanical loading, respectively, and C is a constant. The values of $A, B,$ and C for geopolymer are 49.16, 4.47, and 1.32, respectively. It is stated that the proposed formula is valid only up to 80 °C, beyond which the estimation may not accurate enough.

Eq.5 was then adjusted to calculate the CO_2 permeability, and the values of the material constants A_T and A_P of FA-based geopolymer were evaluated based on the experimental results. The modified equation to predict the permeability of geopolymer at different temperatures is given in Eq. 7.

$$k_T = k_0 10^{0.016(T-T_0)} \left(\frac{P_{in}}{P_{out}}\right)^{0.65} \quad (7)$$

Where P_{in} is the inlet pressure, P_{out} is the downstream pressure given by Eq. 6, and A_T and A_P are 0.016 and 0.65, respectively for fly ash-based geopolymer.

There are a number of theoretical and empirical models developed and progressed to predict the CO_2 permeability in FA-based geopolymer. However, still there are various parameters to be incorporated in the models to accurately predict the permeability values.

6. Meta-analysis with current experimental results on FA-based geopolymer well cement

Through the thorough literature review, the weaknesses of OPC as a well cement were identified, and the suitability of FA-based geopolymers to replace the OPC in geo-sequestration projects is investigated. In this context, the well designers have a responsibility to provide accurate details about mix composition and other preparation conditions for achieving the required properties of FA-based geopolymer to maintain the wellbore integrity at different temperature and pressure variations under downhole conditions.

For encouraging the utilization of FA-based geopolymer as a well cement, apart from comprehensively reviewing pertinent studies, an analytical study was carried out to develop predictive models for dry density, compressive strength, autogenous shrinkage strain**,** and permeability of FA-based geopolymer using different influential parameters. For this purpose, databases were developed by collecting data from many experimental studies available in the literature and using different analytical techniques including Multivariable Regression (MVR) and Artificial Neural Network (ANN) analyses. The mainly used input variables are alkaline activator to FA ratio (AA/FA), Na_2SiO_3 to NaOH ratio (SS/SH), NaOH concentration (M), water to solid ratio (W/S), curing temperature (CT), and curing time (T).

6.1. Predictive model for the dry density of FA-based geopolymer

The developed model predicts the dry density of the FA-based geopolymer mix, considering Na_2SiO_3 to NaOH ratio (SS/SH), alkaline activator to fly ash ratio (AA/FA), and NaOH concentration (M) as influential parameters. 45 data sets were collected from the experimental investigations carried out by Ahdaya & Imqam (2019) and Mermerdaş et al. (2020), in which 34 and 11 data sets were used for model development and model validation, respectively. The developed non-linear multivariable regression model (NL-MVR) is given in Eq. 8, which has a strong coefficient of determination value (R^2) of 0.964, confirming the higher accuracy of the model. The relevant coefficients of the non-linear equation are listed in Table 9.

$$Dry\ Density = -a_1 + a_2\left(\frac{SH}{SS}\right)^b - a_3\left(\frac{AA}{FA}\right)^c - a_4M^d + a_5\left(\frac{SH}{SS}\right)^e\left(\frac{AA}{FA}\right)^f + a_6M^{g\frac{AA}{FA}} - a_7(M)\left(\frac{AA}{FA}\right) \quad (8)$$

Table 9. Coefficients of the nonlinear equation developed for dry density of FA-based geopolymer (refer to Eq. 8)

Coefficient	Value
a_1	31202.079
a_2	513.493
a_3	5302.295
a_4	-55729.
a_5	3664.797
a_6	90213.612
a_7	43.769
b	0.328
c	-0.793
d	0.005
e	0.005
f	-0.968
g	0.01

6.2. Predictive model for compressive strength of FA-based geopolymer

Mainly three different models were developed for predicting the compressive strength of FA-based geopolymer using various input variables, as compressive strength is highly important in preserving the well integrity during the CO_2 sequestration process. Among them, model 1 was developed using ANN due to the complex relationship between the selected input variables and the output variable. The model parameters are given in Annex B. This statistical model can be used to predict the compressive strength of FA-based geopolymer when the alkaline activator to FA ratio (AA/FA), Na_2SiO_3 to NaOH ratio (SS/SH), NaOH concentration (M), curing temperature (CT), and curing time (T) are known. The developed model has an R^2 value of 0.916 which confirms the reasonable accuracy of predicting the compressive strength of FA-based geopolymer.

Model 2 for compressive strength estimation was developed using Si/Al ratio and curing temperature (CT) as independent variables. The data set of FA-based geopolymers with different Si/Al ratios and curing temperatures for the analysis was gathered from a research study that was conducted by Zhou et al. (2016) . The collected data was divided by a 3:1 ratio for model development and validation. The resulting NL-MVR model is a second-degree polynomial equation (refer to Eq. 9) with an R^2 value of 0.976, and it coincides with the findings shown in Figure 13 in section 5.2. In fact, according to the graphical representation presented in Figure 13, the compressive strength rises near-linearly with silica content up to a certain extent, beyond which the compressive strength was reduced with the increment of silica percentage. This behaviour is confirmed by the developed Eq. 9.

$$CS = -1.015 + 0.08615(CT) + 18.4\left(\frac{S}{A}\right) + 0.0002946\,(CT)^2 - 0.01148(CT)\left(\frac{S}{A}\right) - 4.449\left(\frac{S}{A}\right)^2 \quad (9)$$

Where CS is the compressive strength in MPa, CT is the curing temperature in ^{0}C and S/A is the Si/Al ratio in the geopolymer mixture.

From the review, it was identified that developing a model for predicting the compressive strength of FA-based geopolymer with different Water to geopolymer solid ratios (W/S), Curing temperature (CT), and curing time (T) is important to prepare an FA-based geopolymer mixture with required compressive strength characteristics. Hence, model 3 was developed considering these parameters, where 32 samples were collected from the experimental investigation done by Nikolić et al. (2015). Out of the collected 32 data sets, 24 samples were used for the development of the model and 8 samples were used for the validation. Linear multivariable regression (L-MVR) analysis was performed, and a model was developed with an R^2 value of 0.932, which indicates a strong relationship between independent variables and the dependent variable (refer to Eq. 10).

$$CS = -122.2217499\left(\frac{W}{S}\right) + 0.163917701(CT) + 0.358590226(T) + 69.86642578 \quad (10)$$

6.3. Predictive model for autogenous shrinkage strain of FA-based geopolymer

Since prediction of shrinkage of FA geopolymer is important at the primary stage of well cement preparation, an NL-MVR model was developed by using 160 data sets, where 132 and 30 data sets were used to develop and test the model, respectively. This model predicts the autogenous shrinkage strain (ASS) of the FA-based geopolymer mix after the curing period, considering Na_2SiO_3 to NaOH ratio (SS/SH), Age of cement paste (T), NaOH concentration (M) and binder (B) as independent variables. Binder means the mass of fly ash and alkaline activator that is included in m^3 of FA-based geopolymer mixture. The developed NL-MVR model is given in Eq. 11, which has an R^2 value of 0.862. Hence, the developed reasonably accurate model can be used to approximately estimate the autogenous shrinkage of FA-based geopolymer during the pre-feasibility stage of the CO_2 sequestration project.

$$ASS = \left[153.606(M)^{0.862} - 153.094(B)^{0.536} + 30021.428(T)^{0.002} + 0.588(M)\left(\frac{SS}{SH}\right) + 0.025\left(\frac{SS}{SH}\right)(B) + 4.258(B) + 77.402(M) + 13.007(SS/SH) - 28208.902\right] x10^{-6} \quad (11)$$

6.4. Predictive model for CO_2 permeability of FA-based geopolymer

To predict the CO_2 permeability (k) in FA-based geopolymer, five linear multivariable regression (L-MVR) equations were developed using the independent variables as injection pressure (p_i) and curing temperature (T) under different confining pressures including 12, 16, 20, 25, 35 MPa. The developed equations for the selected parameters under each divided group are shown in Eq.12-16.

$$k\,(P_i, T) = \begin{cases} -0.003103851p_i + 0.000459223\,T + 0.017956233; & Pc = 12 \quad (R^2 = 0.880) \quad (12) \\ -0.001069696p_i + 0.000254524T + 0.007122723; & Pc = 16 \quad (R^2 = 0.995) \quad (13) \\ -0.000245848p_i + 0.000124239T + 0.001017792; & Pc = 20 \quad (R^2 = 0.959) \quad (14) \\ -0.003950112p_i + 0.001158095T + 0.050207161; & Pc = 25 \quad (R^2 = 0.964) \quad (15) \\ -0.000391676p_i + 0.000175025T + 0.006027776; & Pc = 35 \quad (R^2 = 0.980) \quad (16) \end{cases}$$

These results further concluded that the linear relationship between injection pressure and the temperature with CO_2 permeability has been strengthened with the increment of confining pressure values. According to the developed equations, CO_2 permeability increases with increasing temperature and decreases with increasing injection pressure under specified confining pressures. The resulting R^2 values for these developed models conclude that the predicted results from these regression models exhibit a reasonable correlation with the experimental values for the selected input parameters.

7. Summary

Well cement plays a major role in the CO_2 sequestration process, where the sealing property of the well cement is highly important to confirm the leakage-free process. With these requirements, the existing research work was generally carried out in different paths, where they have mainly focused on generally used API-class well cement, associated issues with the traditionally used well cement at CO_2 rich environment, leakage pathways of CO_2, the flow and mechanical behaviour changes under

different temperature and pressure variations and the quality of the cement slurry. According to past-observed results, the generally used OPC has shown considerable degradation at downhole conditions, reducing the sealant properties of the well cement. Based on these experimental works, most of the researchers confirmed the inability of OPC to perform in acidic downhole conditions as a stable well cement. In addition to the degradation, the OPC has shown some other weaknesses such as higher shrinkage properties, high permeability and porosity values, and strength reductions.

To address these issues of OPC well cement, inorganic geopolymer was introduced as an alternate solution, where different alumino-silicate source materials were proposed as geopolymers. Due to the ability to reduce the gigantic amounts of fly ash piled up during coal-fired power plant operations, FA-based geopolymer as an alternative well cement has gained vast popularity in the industry. Therefore, the properties of FA-based geopolymer and its applicability as a more effective well cement in the CO_2 sequestration process were examined widely by many researchers.

Through this comprehensive review, major influential parameters of FA-based geopolymer well cement were analysed, mainly focusing on the compressive strength changes under different curing temperatures and various chemical compositions. Further, the other main factor that has influenced the maintenance of required wellbore integrity and zonal isolation is the permeability of bonding material. Therefore, the relevant literature on permeability changes under different mix compositions and temperatures has also been investigated.

From the thorough literature review, it was found that there was no proper representation or relationship developed between the influential parameters and the resultant well behaviour, which confirms the applicability of FA-based geopolymers as an effective well cement. Hence, a meta-analysis was carried out to develop accurate correlations between such parameters. The outcomes of the meta-analysis will be helpful for decision-making regarding the appropriateness of applying FA-based geopolymer as a replacement to OPC in order to conduct a sustainable geo-sequestration process under proper isolation conditions.

8. Recommendations for future work

The main objective of this research study was to investigate FA-based geopolymer well cement during the CO_2 sequestration process, through an analytical and comparative study. A systematic review on the usage of FA as geopolymer material during CO_2 sequestration was conducted and the findings were discussed comprehensively in the 1st phase of the study. In the 2nd phase, statistical models were introduced using MVR analysis and ANN technique. Four important properties of FAG were targeted for the model development including FAG dry density, compressive strength, autogenous shrinkage strain, and CO_2 permeability in FAG. Since there is numerous research being carried out considering different other influential parameters, it is suggested to collect the experimental data and create a database, which can be used to develop more accurate correlations to predict the mechanical behaviour of FA-based geopolymer as well cement for the CO_2 sequestration process. In fact, the density of the FA-based geopolymers varies with the curing type and the conditions; as such, further studies are recommended to improve the developed models by using the densities of the FAG samples that are prepared at different curing conditions. Due to the limited availability of data, three models were developed to predict the compressive strength of FAG using different input variables in each model. It is recommended to develop a single model that represents all the above-mentioned input parameters, which will be more effective in taking direct decisions on the compressive strength of FAG.

9. Statements and Declarations

The authors have no competing interests to declare that are relevant to the content of this article.

10. References

Abdulkareem, O. A, Al Bakri Abdullah, M. M., Kamarudin, H., & Khairul Nizar, I. (2012). *The influence of curing periods on the compressive strength of fly ash-based geopolymer at different aging times*. *479*, 512–516.

Abdulkareem, O. A., & Ramli, M. (2015). Optimization of alkaline activator mixing and curing conditions for a fly ash-based geopolymer paste system. *Modern Applied Science*, *9*(12), 61.

Ahdaya, M., & Imqam, A. (2019). Fly ash Class C based geopolymer for oil well cementing. *Journal of Petroleum Science and Engineering*, *179*, 750–757.

Al Bakri Abdullah, M. M., Kamarudin, H., Abdulkareem, O. A., Ghazali, C. M. R., Rafiza, A., & Norazian, M. (2012). *Optimization of alkaline activator/fly ash ratio on the compressive strength of manufacturing fly ash-based geopolymer*. *110*, 734–739.

Al Bakria, A. M., Kamarudin, H., BinHussain, M., Nizar, I. K., Zarina, Y., & Rafiza, A. (2011). The effect of curing temperature on physical and chemical properties of geopolymers. *Physics Procedia*, *22*, 286–291.

Álvarez-Ayuso, E., Querol, X., Plana, F., Alastuey, A., Moreno, N., Izquierdo, M., Font, O., Moreno, T., Diez, S., & Vázquez, E. (2008). Environmental, physical and structural characterisation of geopolymer matrixes synthesised from coal (co-) combustion fly ashes. *Journal of Hazardous Materials*, *154*(1–3), 175–183.

Backe, K., Lile, O., Lyomov, S., Elvebakk, H., & Skalle, P. (1999). Characterizing curing-cement slurries by permeability, tensile strength, and shrinkage. *SPE Drilling & Completion*, *14*(03), 162–167.

Barlet-Gouédard, V., Rimmelé, G., Porcherie, O., Quisel, N., & Desroches, J. (2009). A solution against well cement degradation under CO2 geological storage environment. *International Journal of Greenhouse Gas Control*, *3*(2), 206–216.

Bertier, P., Swennen, R., Laenen, B., Lagrou, D., & Dreesen, R. (2006). Experimental identification of CO2–water–rock interactions caused by sequestration of CO2 in Westphalian and Buntsandstein sandstones of the Campine Basin (NE-Belgium). *Journal of Geochemical Exploration*, *89*(1–3), 10–14.

Brandvoll, Ø., Regnault, O., Munz, I., Iden, I., & Johansen, H. (2009). Fluid–solid interactions related to subsurface storage of CO2 Experimental tests of well cement. *Energy Procedia*, *1*(1), 3367–3374.

Chindaprasirt, P., Chareerat, T., & Sirivivatnanon, V. (2007). Workability and strength of coarse high calcium fly ash geopolymer. *Cement and Concrete Composites*, *29*(3), 224–229.

Chindaprasirt, P., Jaturapitakkul, C., Chalee, W., & Rattanasak, U. (2009). Comparative study on the characteristics of fly ash and bottom ash geopolymers. *Waste Management*, *29*(2), 539–543.

Cho, Y. K., Jung, S. H., & Choi, Y. C. (2019). Effects of chemical composition of fly ash on compressive strength of fly ash cement mortar. *Construction and Building Materials*, *204*, 255–264.

Condor, J., & Asghari, K. (2009). Experimental study of stability and integrity of cement in wellbores used for CO2 storage. *Energy Procedia*, *1*(1), 3633–3640.

Davidovits, J. (1994). *Properties of geopolymer cements*. *1*, 131–149.

Davidovits, J. (2005). *Geopolymer, green chemistry and sustainable development solutions: Proceedings of the world congress geopolymer 2005*. Geopolymer Institute.

Di Lullo, G., & Rae, P. (2000). *Cements for Long Term Isolation-Design Optimization by Computer Modelling and Prediction*. IADC/SPE Asia Pacific Drilling Technology.

Duguid, A., & Scherer, G. W. (2010). Degradation of oilwell cement due to exposure to carbonated brine. *International Journal of Greenhouse Gas Control*, *4*(3), 546–560.

Fulekar, M., & Dave, J. (1986). Disposal of fly ash—An environmental problem. *International Journal of Environmental Studies*, *26*(3), 191–215.

Gawin, D., Majorana, C., & Schrefler, B. (1999). Numerical analysis of hygro-thermal behaviour and damage of concrete at high temperature. *Mechanics of Cohesive-frictional Materials: An International Journal on Experiments, Modelling and Computation of Materials and Structures*, *4*(1), 37–74.

Goodwin, K. (1997). Oilwell/gaswell cement-sheath evaluation. *Journal of Petroleum Technology*, *49*(12), 1339–1343.

Gunasekara, M. C., Law, D., & Setunge, S. (2014). *Effect of composition of fly ash on compressive strength of fly ash based geopolymer mortar*. 113–118.

Guo, X., Shi, H., & Dick, W. A. (2010). Compressive strength and microstructural characteristics of class C fly ash geopolymer. *Cement and Concrete Composites*, *32*(2), 142–147.

Hardjito, D., Cheak, C. C., & Ing, C. L. (2008). Strength and setting times of low calcium fly ash-based geopolymer mortar. *Modern Applied Science*, *2*(4), 3–11.

Hardjito, D., & Rangan, B. V. (2005). *Development and properties of low-calcium fly ash-based geopolymer concrete*.

Hardjito, D., Wallah, S. áE., Sumajouw, D. áM. J., & Vijaya Rangan, B. (2004). On the development of Fly ash-based Geopolymer concrete. *ACI Materials Journal*.

Helmy, A. I. I. (2016). Intermittent curing of fly ash geopolymer mortar. *Construction and Building Materials*, *110*, 54–64.

Hewayde, E., Nehdi, M., Allouche, E., & Nakhla, G. (2006). Effect of geopolymer cement on microstructure, compressive strength and sulphuric acid resistance of concrete. *Magazine of Concrete Research*, *58*(5), 321–331.

Huber, M. L., Lemmon, E. W., Diky, V., Smith, B. L., & Bruno, T. J. (2008). Chemically authentic surrogate mixture model for the thermophysical properties of a coal-derived liquid fuel. *Energy & Fuels*, *22*(5), 3249–3257.

Huerta, N. J., Bryant, S. L., Strazisar, B. R., Kutchko, B. G., & Conrad, L. C. (2009). The influence of confining stress and chemical alteration on conductive pathways within wellbore cement. *Energy Procedia*, *1*(1), 3571–3578.

Ionescu, B. A., & Lăzărescu, A. (2020). *A Review Regarding the Use of Natural and Industrial by-products in the Production of Geopolymer Binders*. *877*(1), 012033.

Ji, X., & Zhu, C. (2015). CO2 storage in deep saline aquifers. In *Novel materials for carbon dioxide mitigation technology* (pp. 299–332). Elsevier.

Kaldi, J. G., Gibson-Poole, C. M., & Payenberg, T. H. (2009). *Geological input to selection and evaluation of CO2 geosequestration sites*.

Kannangara, T., Guerrieri, M., Fragomeni, S., & Joseph, P. (2021). Effects of Initial Surface Evaporation on the Performance of Fly Ash-Based Geopolymer Paste at Elevated Temperatures. *Applied Sciences*, *12*(1), 364.

Karakurt, I., & Aydin, G. (2023). Development of regression models to forecast the CO2 emissions from fossil fuels in the BRICS and MINT countries. *Energy*, *263*, 125650.

Khalifeh, M., Saasen, A., Vralstad, T., & Hodne, H. (2014). Potential utilization of class C fly ash-based geopolymer in oil well cementing operations. *Cement and Concrete Composites*, *53*, 10–17.

Kiattikomol, K., Jaturapitakkul, C., Songpiriyakij, S., & Chutubtim, S. (2001). A study of ground coarse fly ashes with different finenesses from various sources as pozzolanic materials. *Cement and Concrete Composites*, *23*(4–5), 335–343.

Kong, D. L., Sanjayan, J. G., & Sagoe-Crentsil, K. (2007). Comparative performance of geopolymers made with metakaolin and fly ash after exposure to elevated temperatures. *Cement and Concrete Research*, *37*(12), 1583–1589.

Kovalchuk, G., Fernández-Jiménez, A., & Palomo, A. (2007). Alkali-activated fly ash: Effect of thermal curing conditions on mechanical and microstructural development–Part II. *Fuel*, *86*(3), 315–322.

Krilov, Z., Loncaric, B., & Miksa, Z. (2000). *Investigation of a long-term cement deterioration under a high-temperature, sour gas downhole environment*. SPE International Symposium on Formation Damage Control.

Kutchko, B. G., & Kim, A. G. (2006). Fly ash characterization by SEM–EDS. *Fuel*, *85*(17–18), 2537–2544.

Kutchko, B. G., Strazisar, B. R., Dzombak, D. A., Lowry, G. V., & Thaulow, N. (2007). Degradation of well cement by CO2 under geologic sequestration conditions. *Environmental Science & Technology*, *41*(13), 4787–4792.

Labibzadeh, M. (2010). Assessment of the early age tensile strength of the oilfield class g cement under effects of the changes in down-hole pressure and temperature. *Trends in Applied Sciences Research*, *5*(3), 165–176.

Laudet, J.-B., Garnier, A., Neuville, N., Le Guen, Y., Fourmaintraux, D., Rafai, N., Burlion, N., & Shao, J.-F. (2011). The behavior of oil well cement at downhole CO2 storage conditions: Static and dynamic laboratory experiments. *Energy Procedia*, *4*, 5251–5258.

Lăzărescu, A., Szilagyi, H., Baeră, C., & Ioani, A. (2017). *The effect of alkaline activator ratio on the compressive strength of fly ash-based geopolymer paste*. *209*(1), 012064.

Lécolier, E., Rivereau, A., Le Saoût, G., & Audibert-Hayet, A. (2007). Durability of hardened portland cement paste used for oilwell cementing. *Oil & Gas Science and Technology-Revue de l'IFP*, *62*(3), 335–345.

Mavroudis, D. (2001). Downhole environmental risks associated with drilling and well completion practices in the cooper/eromanga basins. *Report Book*, *9*.

Mermerdaş, K., Algın, Z., & Ekmen, Ş. (2020). Experimental assessment and optimization of mix parameters of fly ash-based lightweight geopolymer mortar with respect to shrinkage and strength. *Journal of Building Engineering*, *31*, 101351.

Mishra, A., Choudhary, D., Jain, N., Kumar, M., Sharda, N., & Dutt, D. (2008). Effect of concentration of alkaline liquid and curing time on strength and water absorption of geopolymer concrete. *ARPN J. Eng. Appl. Sci*, *3*(1), 14–18.

Moon, G. D., Oh, S., & Choi, Y. C. (2016). Effects of the physicochemical properties of fly ash on the compressive strength of high-volume fly ash mortar. *Construction and Building Materials*, *124*, 1072–1080.

Nasvi, Gamage, R. P., & Jay, S. (2012a). Geopolymer as well cement and the variation of its mechanical behavior with curing temperature. *Greenhouse Gases: Science and Technology*, *2*(1), 46–58.

Nasvi, M. M. C., Gamage, R. P., & Jay, S. (2012b). Geopolymer as well cement and the variation of its mechanical behavior with curing temperature. *Greenhouse Gases: Science and Technology*, *2*(1), 46–58. https://doi.org/10.1002/ghg.39

Nasvi, Ranjith, P., & Sanjayan, J. (2013). The permeability of geopolymer at down-hole stress conditions: Application for carbon dioxide sequestration wells. *Applied Energy*, *102*, 1391–1398.

Nasvi, Ranjith, P., & Sanjayan, J. (2014). Effect of different mix compositions on apparent carbon dioxide (CO2) permeability of geopolymer: Suitability as well cement for CO2 sequestration wells. *Applied Energy*, *114*, 939–948.

Nasvi, Ranjith, P., & Sanjayan, J. (2015). A numerical study of triaxial mechanical behaviour of geopolymer at different curing temperatures: An application for geological sequestration wells. *Journal of Natural Gas Science and Engineering*, *26*, 1148–1160.

Nath, S., Mukherjee, S., Maitra, S., & Kumar, S. (2014). Ambient and elevated temperature geopolymerization behaviour of class F fly ash. *Transactions of the Indian Ceramic Society*, *73*(2), 126–132.

Newell, R., Raimi, D., & Aldana, G. (2019). Global energy outlook 2019: The next generation of energy. *Resources for the Future*, *1*, 8–19.

Nikolić, V., Komljenović, M., Baščarević, Z., Marjanović, N., Miladinović, Z., & Petrović, R. (2015). The influence of fly ash characteristics and reaction conditions on strength and structure of geopolymers. *Construction and Building Materials*, *94*, 361–370.

Olivia, M., & Nikraz, H. (2011). *Durability of fly ash geopolymer concrete in a seawater environment*. Proceedings of the CONCRETE 2011 Conference.

Palomo, A., Grutzeck, M., & Blanco, M. (1999). Alkali-activated fly ashes: A cement for the future. *Cement and Concrete Research*, *29*(8), 1323–1329.

Panias, D., Giannopoulou, I. P., & Perraki, T. (2007). Effect of synthesis parameters on the mechanical properties of fly ash-based geopolymers. *Colloids and Surfaces A: Physicochemical and Engineering Aspects*, *301*(1–3), 246–254.

Pedersen, R., Scheie, A., Johnson, C. R., Hoyos, J. C., Therond, E., & Khatri, D. K. (2006). *Cementing of an offshore disposal well using a novel sealant that withstands pressure and temperature cycles*. IADC/SPE Drilling Conference.

Pratt, A., Talman, S., Zhang, M., & Thibeau, Y. (2009). *Characterization of Portland cement reacted with supercritical CO2*. 4–7.

Provis, J. L., Yong, C. Z., Duxson, P., & van Deventer, J. S. (2009). Correlating mechanical and thermal properties of sodium silicate-fly ash geopolymers. *Colloids and Surfaces A: Physicochemical and Engineering Aspects*, *336*(1–3), 57–63.

Raijiwala, D., Patil, H., & Kundan, I. (2012). Effect of alkaline activator on the strength and durability of geopolymer concrete. *Journal of Engineering Research and Studies*, *3*(1), 18–21.

Rangan, B. V. (2008). *Fly ash-based geopolymer concrete*.

Ranjith, P., & Perera, M. (2011). A new triaxial apparatus to study the mechanical and fluid flow aspects of carbon dioxide sequestration in geological formations. *Fuel*, *90*(8), 2751–2759.

Rattanasak, U., & Chindaprasirt, P. (2009). Influence of NaOH solution on the synthesis of fly ash geopolymer. *Minerals Engineering*, *22*(12), 1073–1078.

Rickard, W. D., Williams, R., Temuujin, J., & Van Riessen, A. (2011). Assessing the suitability of three Australian fly ashes as an aluminosilicate source for geopolymers in high temperature applications. *Materials Science and Engineering: A*, *528*(9), 3390–3397.

Ridha, S., Hamid, A. I. A., Setiawan, R. A., Ibrahim, M. A., & Shahari, A. R. (2018). Microstructure behavior of fly ash-based geopolymer cement exposed to acidic environment for oil well cementing. *Arabian Journal for Science and Engineering*, *43*(11), 6413–6428.

Ridha, S., Setiawan, R. A., Pramana, A. A., & Abdurrahman, M. (2020). Impact of wet supercritical CO2 injection on fly ash geopolymer cement under elevated temperatures for well cement applications. *Journal of Petroleum Exploration and Production Technology*, *10*(2), 243–247.

Robins, N., & Milodowski, A. (1986). Borehole cements and the downhole environment—A review. *Quarterly Journal of Engineering Geology and Hydrogeology*, *19*(2), 175–181.

Sagoe–Crentsil, K., Brown, T., & Yan, S. Q. (2010). *Medium to long term engineering properties and performance of high-strength geopolymers for structural applications*. *69*, 135–142.

Sakulich, A. R., Anderson, E., Schauer, C., & Barsoum, M. W. (2009). Mechanical and microstructural characterization of an alkali-activated slag/limestone fine aggregate concrete. *Construction and Building Materials*, *23*(8), 2951–2957.

Sampath, K., Ranjith, P., & Perera, M. (2020). *A Comprehensive Review of Structural Alterations in CO_2-Interacted Coal: Insights into CO_2 Sequestration in Coal*.

Santra, A. K., Reddy, B., Liang, F., & Fitzgerald, R. (2009). *Reaction of CO2 with Portland cement at Downhole Conditions and the Role of Pozzolanic Supplements*. SPE International Symposium on Oilfield Chemistry.

Sarker, P. K. (2011). Bond strength of reinforcing steel embedded in fly ash-based geopolymer concrete. *Materials and Structures*, *44*(5), 1021–1030.

Sauki, A., & Irawan, S. (2010). Effects of pressure and temperature on well cement degradation by supercritical CO2. *International Journal of Engineering & Technology IJET-IJENS*, *1*(04), 53–61.

Shahriar, A. (2011). *Investigation on rheology of oil well cement slurries*.

Shill, S. K., Al-Deen, S., Ashraf, M., & Hutchison, W. (2020). Resistance of fly ash based geopolymer mortar to both chemicals and high thermal cycles simultaneously. *Construction and Building Materials*, *239*, 117886.

Siriwardane, H., Haljasmaa, I., McLendon, R., Irdi, G., Soong, Y., & Bromhal, G. (2009). Influence of carbon dioxide on coal permeability determined by pressure transient methods. *International Journal of Coal Geology*, *77*(1–2), 109–118.

Sofi, M., Van Deventer, J., Mendis, P., & Lukey, G. (2007). Engineering properties of inorganic polymer concretes (IPCs). *Cement and Concrete Research*, *37*(2), 251–257.

Somna, K., Jaturapitakkul, C., Kajitvichyanukul, P., & Chindaprasirt, P. (2011). NaOH-activated ground fly ash geopolymer cured at ambient temperature. *Fuel*, *90*(6), 2118–2124.

Tempest, B., Sanusi, O., Gergely, J., Ogunro, V., & Weggel, D. (2009). *Compressive strength and embodied energy optimization of fly ash based geopolymer concrete*. 1–17.

Thakur, R. N., & Ghosh, S. (2009). Effect of mix composition on compressive strength and microstructure of fly ash based geopolymer composites. *ARPN Journal of Engineering and Applied Sciences*, *4*(4), 68–74.

Thokchom, S., Mandal, K. K., & Ghosh, S. (2012). Effect of Si/Al ratio on performance of fly ash geopolymers at elevated temperature. *Arabian Journal for Science and Engineering*, *37*(4), 977–989.

Uehara, M. (2010). New concrete with low environmental load using the geopolymer method. *Quarterly Report of RTRI*, *51*(1), 1–7.

Van den Heede, P., Gruyaert, E., & De Belie, N. (2010). Transport properties of high-volume fly ash concrete: Capillary water sorption, water sorption under vacuum and gas permeability. *Cement and Concrete Composites*, *32*(10), 749–756.

Xie, J., & Kayali, O. (2014). Effect of initial water content and curing moisture conditions on the development of fly ash-based geopolymers in heat and ambient temperature. *Construction and Building Materials*, *67*, 20–28.

Yang, Z., Ha, N., Jang, M., & Hwang, K. H. (2009). *Geopolymer concrete fabricated by waste concrete sludge with silica fume*. *620*, 791–794.

Zain, M. F. M., Mahmud, H., Ilham, A., & Faizal, M. (2002). Prediction of splitting tensile strength of high-performance concrete. *Cement and Concrete Research*, *32*(8), 1251–1258.

Zhang, M., & Talman, S. (2014). Experimental study of well cement carbonation under geological storage conditions. *Energy Procedia*, *63*, 5813–5821.

Zhou, W., Yan, C., Duan, P., Liu, Y., Zhang, Z., Qiu, X., & Li, D. (2016). A comparative study of high- and low-Al 2 O 3 fly ash based-geopolymers: The role of mix proportion factors and curing temperature. *Materials & Design*, *95*, 63–74. https://doi.org/10.1016/j.matdes.2016.01.084

Annex A

Table A.1. A summary of literature on chemical composition of FA in different countries

Reference	Country	Power plant	Fly ash type	SiO_2	Al_2O_3	Fe_2O_3	CaO	MgO	K_2O	Na_2O	SO_3	LOI
(Nasvi et al., 2012b)	Australia	Gladstone (Queensland, Australia)	Class F	48.3	30.5	12.1	2.8	1.2	0.4	0.2	0.3	1.7
(Gunasekara et al., 2014)		Gladstone (GFA)	Class F	50.82	29.89	10.26	3.24	0.8	0.58	0	0.28	
		Port Augusta (PAFA	Class F	49.97	31.45	3.22	5.03	1.54	1.87	1.85	0.33	
		Collie (CFA)	Class F	52.67	29.6	11.27	0.94	0.72	0.65	0	0.48	
		Mount Piper (MPFA)	Class F	65.18	25.3	1.9	0.63	0	3.65	0	0.23	
		Tarong (TFA)	Class F	73.12	21.5	1.36	0.29	0	0.63	0	0	
(Provis et al., 2009)		Gladstone Power Station in Queensland	Class F	46.4	28.3	11.7	5.1	1.4	0.6	0.3	0.3	3.3
(Rickard et al., 2011)		Collie power station in Western Australia,	Class F	51.38	26.9	13.2	1.74	1.41	0.9	0.41		1.15
		Eraring power station in New South Wales	Class F	65.47	23	4.03	1.59	0.51	1.68	0.56		1.37
		Tarong power station in Queensland	Class F	73.68	22.4	0.64	0.08	0.17	0.53	0.09		0.79
(Shill et al., 2020)		Eraring thermal power plant	Class F	62.19	27.15	3.23	1.97	0.4	0.89	0.3	0.07	1.75
(Xie & Kayali, 2014)		Eraring thermal power station	Class F	59.6	29.1	3.3		0.4	0.48	0.28	0.2	

(Nasvi et al., 2014)	India	Kolaghat Thermal Power Station	Class F	56.01	29.8	3.58	2.36	0.3	0.73	0.61		0.4
(Nath et al., 2014)		Tata Power, Jojobera plant, Jamshedpur	Class F	52.6	26.55	5.29	5.1	1.76	1.12	0.61		3.1
(Hardjito et al., 2008)	Malaysia	Sejingkat Power Plant in Kuching, Sarawak	Class F	59.9	24.7	6.3	2	1.9	2.9	0.3	0.1	0.3
(Al Bakri Abdullah et al., 2012)		Sultan Abdul Aziz power station	Class F	52.11	23.59	7.39	2.61	0.78	0.8	0.42	0.49	
(Abdulkareem & Ramli, 2015)		Manjung Power Station	Claas C	26.4	9.25	30.13	2.16	0.27	2.58		1.3	3.02
(Abdulkareem et al., 2012)		Sultan Abdul Aziz Power Station	Class F	52.11	23.59	7.39	2.61	0.78	0.8	0.42	0.49	5.59
(Al Bakria et al., 2011)		Manjung power station	Class F	52.11	23.59	7.39	2.61	0.78	0.8	0.42	0.49	
(Nikolić et al., 2015)	Sebia	FA Morava, TPP Morava, Svilajnac.	Class F	55.23	21.43	7.42	7.94	2.61	1.35	0.64	0.81	1.66
		FA Kolubara, TPP Kolubara	Class F	62.13	17.2	5.95	5.67	2	1.04	0.58	0.67	2.88
		FA Kostolac B1, TPP Kostolac	Class F	46.85	23.2	12.14	8.26	2.77	0.81	0.4	1.48	3.44
(Álvarez-Ayuso et al., 2008)		Spanish power plants	Class F	54.1	23.3	8.5	3.5	2	3.2	0.9	0.4	2
		Spanish power plants	Class F	43.4	25.9	19	5.3	1.2	1.2	0.1	0.9	1.5

	Spain	Spanish power plants	Class F	58.1	22.7	6.1	3.5	1.8	1.6	0.6	0.2	3.5
		Spanish power plants	Class F	51.3	25.5	6.9	2.9	1.8	3.6	0.7	0.5	5
(Kovalchuk et al., 2007)		Spanish power plant	Class F	54.42	26.42	7.01	3.21	1.79	3.02	0.59	0.01	2.19
(Palomo et al., 1999)	United States	Pennsylvania Power and Light Co.'s Montour County power plant	Class F	53.2	26	7.95	3.57	0.97	2.59	0.29		2.22
(Panias et al., 2007)	Greece	Greek Public Power Corporation S.A	Class F	48.95	18.61	7.99	10.91	2.76	1.73	0.8	4.11	
(Lăzărescu et al., 2017)	Romania	Mintia power plant	Class F	53.61	26.16	7.58	2.42	1.49	2.6	0.59	0.26	3.57
(Zhou et al., 2016)	China	Shenhua Junggar Energy Corporation in Junggar	Class F	52.4	18.09	0.42	0.33	0.02	0.19	0.03		20.59
(Thokchom et al., 2012)		plant in Shanxi Province	Class F	52.79	20.95	7.76	6.95	3.42	0.51	0.09		
(Helmy, 2016)	Egypt	Geos, Cairo	Class F	55.819	28.112	7.488	2.71	0.846	1.515	0.215	0.344	
(Cho et al., 2019)			Class F	55.4	22.2	6.84	5.12	1.84	1.55	1.26	0.71	3.7
			Class F	59.1	20	6.22	3.65	1.71	1.62	0.99	0.36	4.43
			Class F	62.6	20	7.13	2.83	1.2	1.2	0.65	0.32	2.62
			Class F	54	22	6.43	4.76	1.48	1.21	1.34	0.5	6.7
			Class F	62.4	17.7	6.89	4.15	1.55	0.97	1.24	0.34	2.53

	South Korea		Class F	62.3	19	6.3	3.42	1.49	1.62	0.75	0.37	3.55
			Class F	57.7	21.1	6.39	4.26	1.8	1.67	1.06	0.52	3.91
			Class F	53	20.7	6.94	6.17	2.31	1.21	2.3	0.51	4.93
			Class F	56.6	20.9	8.09	4.66	1.82	1.2	1.27	0.72	2.61
			Class F	58.3	20.8	6.83	3.44	1.39	1.15	0.94	0.35	5.16
			Class F	60	19.8	6.41	3.14	1.32	1.18	0.9	0.49	4.76
			Class F	61.9	18.7	6.15	3.28	1.33	1.19	0.81	0.48	4.43
			Class F	62.3	20.2	6.66	2.54	1.15	1.18	0.64	0.42	3.28
			Class F	52.2	22.4	7.57	5.22	1.93	1.12	1.46	0.82	5.16
			Class F	57.5	20.5	7.16	5.07	1.72	1.43	0.78	0.71	2.75
			Class F	52.4	23	8.85	5.51	2.06	0.79	1.26	0.47	2.94
(Moon et al., 2016)			Class F	53.04	21.38	5.77	3.1	1.41	1.45	0.61	0.2	
			Class F	39.87	18.2	8.07	6.49	1.67	1.17	1.56	0.4	
			Class F	39.62	14.08	6.07	4.94	1.6	1.17	1.12	0.37	
			Class F	41.53	15.16	6.87	5.8	2.13	1.08	0.65	0.43	
			Class F	39.1	16.06	6.82	5.45	1.8	1.73	1.06	0.43	
			Class F	49.91	16.73	6.01	3.9	1.46	1.14	0.04	0.24	

(Kiattikomol et al., 2001)	Thailand		Class F	46.25	26.43	10.71	7.61	2.21	3.07	1.11	1.85	0.23
			Class F	45.02	36.21	4.09	3.64	0.54	0.31	0.44	0.48	5.32
			Class F	43.92	36.62	3.97	3.05	0.55	0.44	0.38	0.64	7.52
			Class F	47.39	22.73	6.29	8.36	2.64	2.95	0.63	3.38	3.12
			Class F	49.04	37.91	2.75	1.03	0.39	0.52	0.38	0.18	4.7
(Somna et al., 2011)		Mae Moh power plant	Class C	31.2	18.9	16.5	20.8	1.86	2.8	1.53	4.1	1.8
(Rattanasak & Chindaprasirt, 2009)			Class C	39.5	19.5	14.1	17.3	1.3	2.9	1.3	2.6	0.8
(Chindaprasirt et al., 2009)			Class C	38.7	20.8	15.3	16.6	1.3	2.1	1.3	2.6	0.8
(Chindaprasirt et al., 2007)			Class C	38.7	20.8	15.3	16.6	1.5	2.7	1.2	2.6	0.1

1

Annex B

Table B.2. Model parameters used for the ANN model.

Parameter	Value
Number of input neurons	5
Number of output neurons	1
Number of hidden layers	1
Number of hidden neurons	8
Number of training epochs	602
Number of total datasets	86
Number of training datasets	71
Number of validation datasets	15
Network type	Feed-forward back-propagation
Transfer function	TANSIG
Error (Performance) function	MSE
Training function	TRAINLM
Adaptation learning function	LEARNGDM

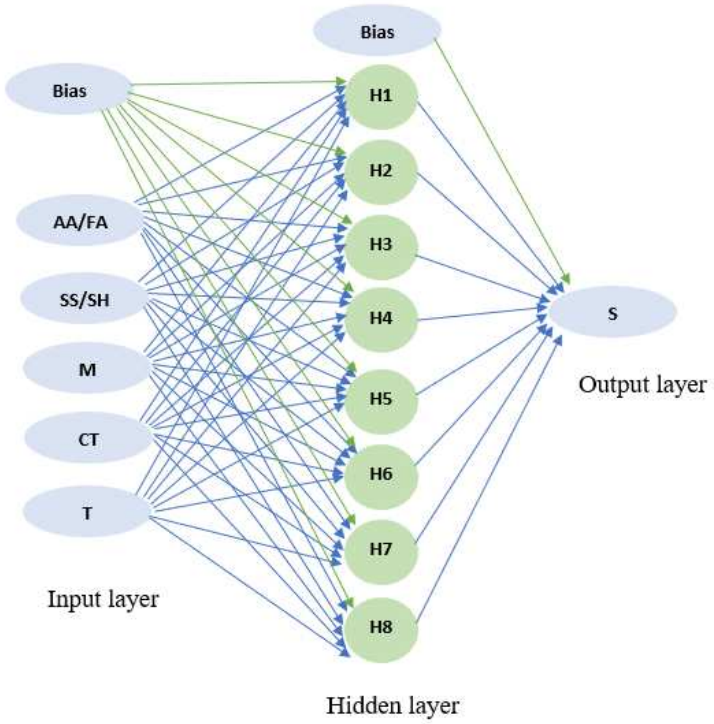

Figure. B.1. Network architecture of the ANN model.